ACTIVE VIBRATION CONTROL OF ROTATING COMPOSITE SHAFT SYSTEM

A THESIS SUBMITTED IN THE PARTIAL FULFILLMENT OF THE REQUIREMENTS FOR THE DEGREE OF

Master of Technology

In

MECHANICAL ENGINEERING

[Specialization: Machine Design and Analysis]

By

Sikandar Kumar

211ME1158

Under the Supervisions of

Prof. T. Roy

Department Of Mechanical Engineering

National Institute of Technology Rourkela

Rourkela, Orissa, India – 769008

December, 2013

Abstract

Fiber reinforced polymer (FRP) composites shafts find many application in the modern industries due to its flexibility and light weight. The present work deals with the study of finite element analysis and active vibration control of rotating composite shaft system under unbalance forces using three nodded beam element. The composite shafts are modeled as a Timoshenko beam by mounting discrete isotropic rigid disks on it and supported by flexible bearings that are modeled with viscous dampers and springs. Based on first order shear deformation (FOSD) beam theory with transverse shear deformation, rotary inertia, gyroscopic effect, strain and kinetic energy of shafts are derived by adopting three-dimensional constitutive relations of material. The derivation of governing equation of motion is obtained using Hamilton's principle and solutions are obtained by three-node finite element (FE) with four degrees of freedom (DOF) per node. Active vibration control of the rotating composite shaft has also been implemented using electromagnetic actuator and PD control technique. Various results have also been obtained such as Campbell diagram, transverse displacements, transverse control responses, control currents and control forces in the both directions. The effect of ply orientation on the Campbell diagrams and the transverse responses has also been studied. The effect of number of actuators on the control responses and the control forces has also been presented.

Keywords: FRP composite shaft, Finite element modeling, Vibration analysis, Electromagnetic actuators, PD control scheme and Active vibration control.

Contents

LIST OF FIGURES

LIST OF TABLES

NOMENCLATURES

$u_{x,}$	Flexural displacements of any point on the cross-section of the shaft in the *x* direction.
u_y	Flexural displacements of any point on the cross-section of the shaft in the *y* direction.
u_z	Flexural displacements of any point on the cross-section of the shaft in *z* direction.
$[M]$	Inertia matrix of rotor shaft bearing system
$[D]$	Combined damping including gyroscopic effect, direct damping of internal material damping, shaft bearing damping
$[K]$	Combined shaft stiffness, bearing stiffness, circulatory effect of the internal material damping of shaft
$\{q\}$	Nodal displacement vector for the entire system
$\{f\}$	Global force vector due to unbalance
$\{f_{EMA}\}$	Force due to electromagnetic actuator
μ_o	Magnetic permeability of free air
A_p	Pole face area, m^2
N	No. of coil turns
i	Current, A
i_o	Bias current, A
g_o	Nominal radial air gap between stator poles and rotor, m
l_g	Length of magnetic flux lines through air gap, m
α	Half of the angle between two adjacent poles
T	Time, s
F_Y, F_Z	Linearized magnetic force along *Y* and *Z* direction, N
F_{Ymag}, F_{Zmag}	Magnetic force along *Y* and *Z* direction, N
K_M	Characteristic constant for a pair of poles in the exciter
K_y, k_z, k_s	Force displacement factor for magnetic exciters, N/m
k_g	Power amplifier gain, A/V
ki	Force current factor, N/A

kp	Gain of displacement feedback sensor, V/m
kv	Gain of velocity feedback sensor, V.s/m
V, w	Translational displacement of a point of a point on rotor along Y and Z axes, respectively, m
J	Cost function
K_{opt}	Optimal gain of LQR
I_{cy}	Control current in Y direction
I_{cz}	Control current in Z direction
$[Q]$	Semi-positive-definite matrix
$[R]$	Positive-definite matrix
F_{YC}, F_{ZC}	Control force along Y and Z directions, N

CHAPTER 1

INTRODUCTION

Rotating composite shaft play an important role in many different industries. Such as in power production, turbines, and aircraft engines, process machines in heavy industry, fans, pumps and ship engines. Now a day Composite rotor shaft materials are being increasingly used. This is due to their good characteristics such as the high strength to mass ratio, the high stiffness to mass ratio, good damping capacity and better resistance to fatigue. Composite materials made of the stiff continuous or long fibers imbedded in soft matrix are used in the structural components which give higher strength and stiffness but weight is lesser. In engineering applications, however, the use of composite materials containing discrete reinforcements may be warranted in order to reduce the cost, make parts of complicate shapes, etc. Composites are formed by combining two or more materials to produce a new material that retains important properties from the original components. These unique combinations deliver significant advantages over traditional materials in structural applications. FRP Composites consist of a polymer matrix material that is reinforced with fibers. The reinforcing fibers provide the primary structural performance of the material, with the polymer transferring the load from fiber-to-fiber and protecting the fibers from the operating environment. Reinforcement may be continuous fibers, discontinuous fibers. Fiber Reinforced Polymer (FRP) composite overturn our society and impinging our daily lives to use that, which are lighter, more durable and have infinite design flexibility.

Vibration in the rotor–shaft–bearing systems is very important in industries, as it creates operational difficulties, inaccuracies, power loss, fatigue and even failure of the system. Reduction of rotor vibration is very important for safe and efficient functioning of all rotor shaft system machines. Active vibration control is the active application of force in which an equal and opposite forces imposed by external vibration. Active vibration control system uses several components. A PID controller can be used to get better performance than a simple inverting amplifier.

There are various types of active material such as: (1) thermo elastic material (2) piezo electric material (3) Magneto-strictive materials (4) electromagnetic actuator (5) micro fiber carbon.

In our present work electromagnetic actuator is used as an active material to control the vibration of composite rotor shaft system in which exciters are mounted on the stator at a plane around the rotor shaft for applying suitable force of actuation over an air gap to control transverse vibration as shown in Fig. 1.1. Perini E. A. et al. [1] developed electromagnets which is used for vibration control do not levitate the rotor and facilitate the bearing action, which is provided by conventional bearings. Suitable force of actuation is achieved by varying the control current in the exciters depending upon p-d control law applied to the displacement of the rotor section with respect to the non-rotating position of the section taken as the

reference. Thus this technique provides control force over an air gap and hence this technique is free from the difficulties of maintenance, wear and tear and power loss. Electromagnetic force is non-linear in nature which is very complex. Hence linearized expression of electromagnetic force is used for finite element analysis. This application shows good reduction in transverse response amplitude, postponement of instability caused by viscous form of rotor internal damping as well as great reduction of support forces.

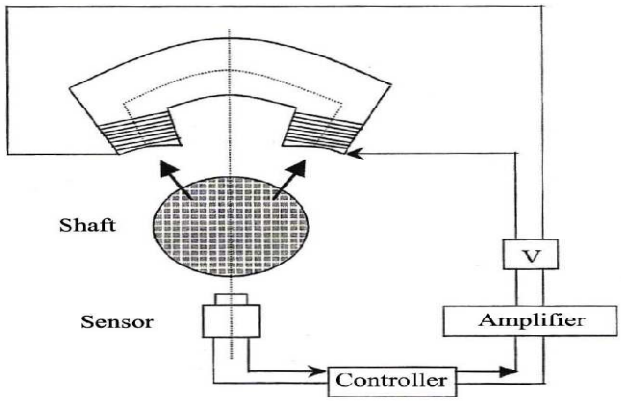

Fig. 1.1: Electro Magnetic levitation principle [1]

Thus this technique provides uncontact type control force over an air gap and hence it is free from the difficulties of maintenance, wear and tear and power losses. There are many control strategy such as PD control, PID control and LQR is used to control the unbalance response of the composite rotor shaft system.

1.1 Composite Materials

Composite Materials can be defined as a combination of two or more dissimilar materials having a distinct interface between them such that the properties of the resulting materials are superior to the individual constituting components. That is insoluble in each other and differs in form or chemical composition.
In other words composite material consists of two or more phase. Two phase composite materials are classified as: (1) Particulate composite and (2) Fiber reinforced composite.

1.1.1 Particulate composite

Particulate composites are having various shape and size which are dispersed within a matrix in a random fashion. Due to this, these composites are treated as quasi-homogeneous and quasi-isotropic. Particulate composites are made of tungsten and molybdenum particles dispersed in silver and copper matrices. It is used for electrical application. Example of particulate composite is mica flakes reinforced with glass, aluminium particles in polyurethane rubber, lead particles in copper alloys etc.

1.1.2 Fiber reinforced composite

Fiber reinforced composite material consist of fibers of significant strength and stiffness embedded in a matrix. Both fibers and matrix maintain their physical and chemical properties. Fiber reinforced composite having continuous fibers are more efficient. FRP can be classified into four categories according to matrix used such as: polymer matrix composites, metal matrix composites, ceramic matrix composite and carbon/carbon composites.

Fiber reinforced composites possess high strength and stiffness. Some material performs equally or better than many traditional metallic materials. Fatigue strength to weight ratio as well as fatigue damage tolerance of many composite laminates is excellent. Coefficient of thermal expansion of FRP composites is much lower than metals.FRP composites possess high internal damping. This leads to better vibration energy absorption within the material, and results in reduced transmission of noise, vibration.

A FRP laminate consists of a series of laminae or plies that are bonded together to act as integral structural element. Each plies are oriented at different angle to produce different strength and stiffness in the required direction of laminate. A lamina or a ply is formed by combining more no. Of fibers in a thin layer of matrix and a laminate is formed by stacking several laminas. It is the most common form of fiber reinforced composites.

1.1.3 Types of Laminates

There are different types of Laminates such as: Symmetrical laminates, balanced laminate, Anti-Symmetrical laminates, Quasi-Isotropic laminate.

1.1.3.1 Symmetrical laminate

A laminates is termed as symmetric when the plies on one side of reference plane are identical to another side in terms of thickness, orientation, properties and position. Also both geometry and material properties should be same about the reference plane. It may contain odd or even number of plies. The plies can all be of single composite or made of hybrid.

An example: $[90_2|45_2|-45_4|45_2|90_2]$ or $[90_2|45_2|-45_2]_s$

The laminate above is symmetric.

Symmetric laminates are of four types as: symmetric laminates with isotropic plies, symmetric laminates with specially orthotropic plies (symmetric cross-ply laminates), symmetric laminates with generally orthotropic layers (symmetric angle-ply laminates), symmetric laminates with anisotropic layers.

1.1.3.2 Balanced Laminate

A laminates is termed as balanced if it contains pair of layers with identical thickness and elastic properties, but the fibers are placed with orientation of $+\theta$ and $-\theta$ with respect to the reference axes. The need not be placed at the same distance from the reference plane.

A balanced laminate may be of any of the three types: symmetric, anti-symmetric or asymmetric.

1.1.3.3 Anti-symmetrical laminate

An anti-symmetric laminate is made up of a number of plies in such a way that for each ply below the middle surface, there is a ply at the same distance above it having identical thickness and material properties, but opposite ply angle. Anti-symmetric laminates are special case of balanced laminates.
There are two types of anti-symmetric laminates as: Anti-symmetric cross-ply laminates, Anti-symmetric angle-ply laminates.

1.1.3.4 Quasi-Isotropic laminate

Quasi-isotropic laminates are combination of specially and generally orthotropic plies. The result is that the inplane stiffnesses and compliances and engineering elastic constant identical in all direction.With the help of orthotropic laminate, it can manufacture which exhibits some elements of isotropic behaviour. Some examples of Quasi-isotropic laminates are:
$[60|-60|0]_s$, $[-45|0|45|90]_s$, $[0/-45/45/90]_s$

1.1.4 Application areas of composites

Fiber reinforced composites have many areas in which it is used such as commercial and industrial. The main application areas may be broadly classified as follows:

- Aircraft and space
- Autpmotive
- Sporting goods
- Marine field
- Civil engineering structures

1.2 Active Material

There are various types of active material such as: (1) Piezo electric material (2) Magneto-strictive materials (3) Electromagnetic actuator (4) Mircro carbon fiber.

1.2.1 Piezoelectric material

Piezoelectric materials develop charge if deformed by mechanical stress. The current generation of piezoelectric materials is generally synthesized with polymeric fibrous composite laminates which readily accommodate piezoelectric actuators and sensors. The inverse effect in piezoelectricity deformation will occur due to the application of an electrical field. External force applied on the structure will set vibrations and cause deformations in the structure. These deformations will cause stresses and strains in the structure. If the structure is embedded with smart crystals, the effects of the vibration can be controlled using a feedback

mechanism. Since piezoelectric undergoes surface elongation, when an electric field is applied and produces charge when surface strain is applied. They can be used as both actuators and sensors. Some commonly used actuation materials are lead zirconate titanate and polyvinylidenefluoride.

1.2.2 Magneto-strictive materials

Magnetostriction material has property of ferromagnetic material. Due to this, its shape or dimension changes during the magnetization. This variation of magnetization due to applied magnetic field will change the magnetostrictive strain until reaching the saturation state. Magnetostriction is mostly found in the materials like iron, cobalt and nickel. Also it is found in the rare earth materials like lanthanum and terbium. The grains of above materials consist of numerous small randomly oriented magnetic constituent, which can be rotated and aligned under the influence of magnetic field.

1.2.3 Electromagnetic actuator

Electromagnetic actuator is specially design as electromagnet that consists of a coil and a movable iron core called the armature. When current flows through a coil, a magnetic field is generated around the coil. When the coil of the solenoid is energized with current, the core moves to increase the flux linkage by closing the air gap between the cores. The movable core is usually spring-loaded to allow the core to retract when the current is switched off. The force generated is approximately proportional to the square of the current and inversely proportional to the square of the length of the air gap.

1.3 Control technique

There are various types of control technique such as:
(1) PD Control,
(2) PID Control and
(3) LQR

1.3.1 PD Controller

Fig.1.2 represents the block diagram of PD control with feedback. The stability and overshoot problems that arise when a proportional controller is used at high gain can be achieve by adding a term proportional to the time-derivative of the error signal. The value of the damping can be adjusted to achieve a critically damped response. PD controllers are slower than P, but less oscillation, smaller overshoot/ripple, Bennett et al. [20]

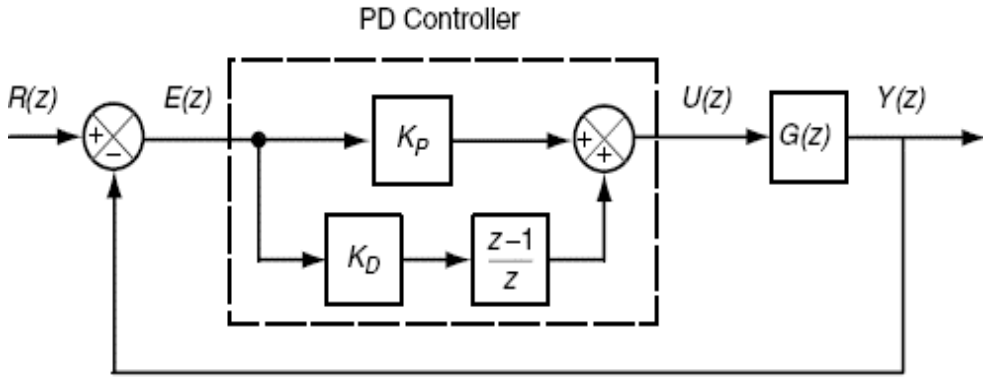

Fig. 1.2: Block diagram of PD controller with feedback [2]

1.3.2 PID Controller

A PID controller calculates an "error" value as the difference between a measured value and a desired set point. The PID controller involves three separate constant parameters, the proportional, the integral and derivative denoted by P, I, and D. The controller is used to minimize the error by adjusting the process control inputs. P depends on the present error, I on the past errors, and D is on future errors, based on current rate of change. In the absence of knowledge of the underlying process, a PID controller has historically been considered to be the best controller. By tuning the three parameters in the PID controller algorithm, the controller can provide control action designed for specific process requirements K.H. Ang et al. [21].

The response of the controller can be described in terms of the responsiveness of the controller to an error, the degree to which the controller overshoots the set point, and the degree of system oscillation. Note that the use of the PID algorithm for control does not guarantee optimal control of the system or system stability.

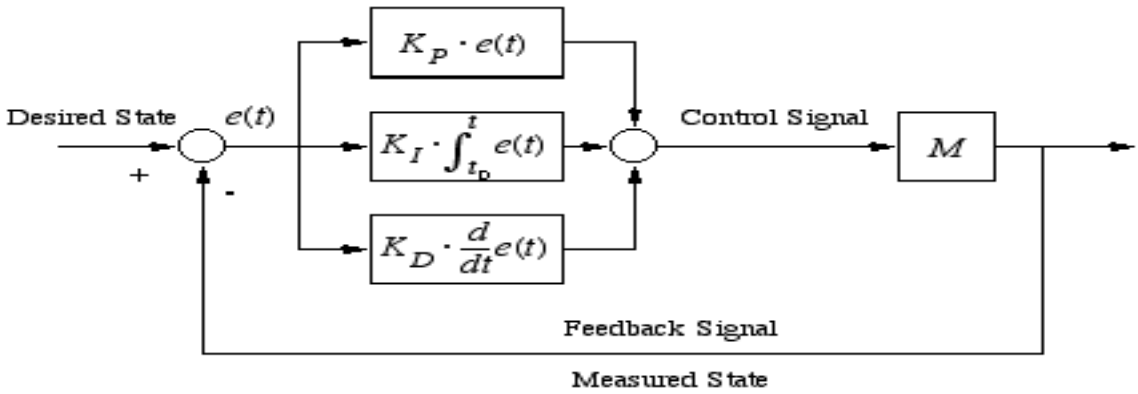

Fig. 1.3: Block diagram of PID controller [3].

$$\mathrm{u}(t) = \mathrm{MV}(t) = K_p e(t) + K_i \int_0^t e(\tau)\,d\tau + K_d \frac{d}{dt} e(t)$$

Where,

K_p= Proportional gain, K_i= Integral gain, K_d= Derivative gain, τ: Variable of integration, e: Error, t: Time

1.3.3 Linear Quadratic Regulation (LQR)

LQR optimal control theory is used to determine the control gains. In this, the feedback control system has been designed to minimize a cost function or a performance index, which is proportional to the required measure of the system's response.

Consider a state-space representation of the equations of motions of an N-DOF linear system. State-space model can be written as-

$$\dot{X} = A * X + B * U(t)$$

The cost function used in the present case is given by

$$J = \frac{1}{2}\int_{t_0}^{t_f} \left(\{X\}^T [Q] \{X\} + \{U\}^T [R] \{U\} \right) dt$$

Where [Q] and[R] are the semi-positive-definite and positive-definite weighting matrices on the outputs and control inputs, respectively.

1.4 Advantages of electromagnetic actuator

There are following advantages of electromagnetic actuator:

- No mechanical wear and friction due to non-contact operation.
- No lubrication, and therefore non-polluting.
- Low energy consumption.
- Operation in severe environments.
- Active vibration control and easy passing of critical speeds.

1.5 Finite element method

Finite element method (FEM) is a numerical method for solving a complex differential or integral equation. It has been applied to a various number of physical problems, where the governing differential equations (it may be linear or non-linear) are available. The method essentially consists of assuming the elementary (i.e. no. of pieces) continuous function for the solution and obtaining the functions so that it reduces the error in the solution. In our present work finite element method has been used for composite rotor shaft system.

1.6 Outline of the Present Work

The outline of this thesis is divided into six chapters.

Chapter 1 represents an introduction of composite material, active material, and control technique also brief introduction to rotor shaft system. The outline of the present work is also given in the Chapter 1.

In Chapter 2 presents literature review on vibration control of isotropic rotor shaft system, vibration control of composite rotor shaft system and, active vibration control of rotor shaft system systems.

In Chapter 3 represents the finite element modelling and analysis of FRP composite shaft system

Chapter 4 presents a modeling and analysis of electromagnetic actuator, governing equations of motion, control strategy.

Chapter 5 discusses the results for many stacking sequence of laminated composite and detailed report of results and discussion has been given.

Chapter 6 summarizes conclusions of this project work and scopes for further work are suggested.

CHAPTER 2

LITERATURE REVIEW

2.1 General Introduction

Based on above research field many researchers have been presented about finite element modelling and vibration analysis of isotropic as well as composite shafts system and active vibration control of rotating shaft considering isotropic materials are also presented in some important literature. These have been in the following sub section

2.2 Finite element modelling and vibration analysis of isotropic shaft system

Vibration caused by mass unbalance is a common problem in rotating shaft. Rotor unbalance occurs when the principal inertia axis of the rotor does not coincide with its geometrical axis and leads to synchronous vibrations and significant undesirable forces transmitted to the mechanical elements and supports. Many researchers have been worked to reduce the vibration caused by unbalance response.

Foeppl [4] developed an analytical method of the dynamic behaviour of the isotropic de Laval rotor. Rotor dynamics as a subject first appeared in the last quarter of the 19th Century due to the problems associated with the high speed turbine of Gustaf de Laval who invented the elastically supported rotor, called de Laval Rotor, and observed its supercritical operation. Foeppl explained analytically the dynamic behaviour of the de Laval rotor. Serious research on rotor dynamics started in 1869 when Rankine published his paper on whirling motions of a rotor. However, he did not realize the importance of the rotor unbalances and therefore concluded that a rotating machine never would be able to operate above the first critical speed. De Laval showed around 1900 that it is possible to operate above critical speed, with his one-stage steam turbine.

Stodola [5] Presents the influence of gyroscopic effects on a rotating system was presented in 1924 by Stodola. The model that was presented consists of a rigid disk with a polar moment of inertia, transverse moment of inertia and mass. The disk is connected to a flexible mass-less overhung rotor. The gyroscopic coupling terms in Stodola's rotor model resulted in the natural frequencies being dependent upon the rotational speed. Jeffcott [6] developed the first paper where the theory of unbalanced rotors is described. Jeffcott derived a theory which shows that it is possible for rotating machines to exceed the critical speeds. However, in the Jeffcott model the mass is basically represented as a particle or a point-mass, and the model can't correctly explain the characteristics of a rigid-body on a flexible rotating shaft R.G. Kirk, et al. [7] analyzed he dynamic unbalance response and transient motion of the single mass Jeffcott rotor in elastic bearings mounted on damped, flexible supports are discussed. A steady state analysis of the shaft and the bearing housing motion was made by assuming synchronous precession of the system. The conditions under which the support system would act as a dynamic vibration absorber at the rotor critical speed were

studied. Lateral vibrations in rotor systems have been analysed extensively by Tondl, Fritz, and Lee, They considered different types of rotor systems, and in all those systems, lateral vibrations are induced by the mass unbalance in a rotor. In all the systems considered it is noticed that increase of mass unbalance can have destabilising effects. For example, Tondl, and Lee, considered a simple disk with a mass unbalance connected to a shaft which is elastic in the lateral direction and found out that in such systems, under certain conditions, instabilities can appear if the mass unbalance increases.

He formed an expression for the work done in a small relative displacement by all forces and obtained the differential equations by way of the calculus of variations. Solutions of the differential equations of motion for an elastic solid were treated by Poisson who founded the general theory of vibrations. The development of vibration theory, as a subdivision of mechanics, came as a natural result of the development of the basic sciences it draws from, mathematics and mechanics. Pythagoras of Samos conducted several vibration experiments with hammers, strings, pipes and shells. He established the first vibration research laboratory. That for a (linear) system there are frequencies at which the system can perform harmonic motion was known to musicians but it was stated as a law of nature for vibration systems by Pythagoras. Moreover, he proved with his hammer experiments that natural frequencies are system properties and do not depend on the magnitude of the excitation.

Nelson et.al [8] presented the Rayleigh beam theory to model the rotor shaft taking into consideration the presence of viscous form of internal material damping, which is caused to instability above the first critical speed.it presented a procedure for dynamic modelling of rotor bearing systems which consisted of rigid disks, distributed parameter finite rotor elements, and discrete bearings. They presented their formulation in both a fixed and rotating frame of reference They developed a finite element model including the effects of rotary inertia, gyroscopic moments. Yamamoto [9] developed rotor-bearing systems in which there are many sources of nonlinearities, such as play in bearings and fluid dynamics in journal bearings. The dynamic stiffness of the bearing which supports the rotating shaft has a significant effect on the vibration. In particular it affects the machine critical speeds and the vibration in between critical speeds suggested that rolling bearings, which are frequently used in industry, sometimes have nonlinear spring characteristics due to coulomb friction and the angular clearance between roller and ring. Holmes et al. [10] Analyzed a paper dealing with a periodic behaviour in journal bearings. In their work, the symmetrical, steady state motion of a rigid shaft supported by two short journal bearings was studied. The behaviour of this test rig was found to be of two distinct types. For small eccentricity, the motion was asymptotically periodic and consisted of a small number of components, principally at synchronous and half-synchronous frequencies. For high eccentricity, the motion observed was complex and did not settle to a limit cycle, remaining in a state of

Panda et.al [11] analyzed the viscoelastic support and their ability to provide good support elements to rotor shaft systems by virtue of their efficiency in dissipating vibratory energy. They studied that the in-phase stiffness and loss factor for such materials also change with the frequency of excitation they are subjected to. They found the frequency dependent characteristics of the polymeric supports by simultaneously minimizing the unbalanced response and maximizing the stability limit speed (SLS). Optimum characteristics have been

found for the rotor shaft system mounted on (a) rolling element bearings and (b) plain cylindrical journal bearings at the ends having polymeric supports. The effects of viscous internal damping in the shaft, support mass and gyroscopic effect due to non-symmetrical location of the disc have been considered in the analysis. A procedure of controlling a slope of the support characteristics versus frequency of excitation has been used and found to be very suitable for obtaining feasible support characteristics.

Cunningham [12] developed a Rotor systems have been traditionally supported on oil-film bearings due to their robustness. The oil-film bearings introduce some damping to the rotor system, but can also lead to oil whip instability. In order to control the resonance and to delay the onset of instability, passive devices such as squeeze-film bearings have been used to augment the system damping. Stanway et al. [13] presented a paper in which supercritical systems has several lateral bending modes of vibration are liable to be excited, and given a single passive device it is not possible to select the stiffness and damping parameters so as to exert a significant influence over all these modes and on the other hand, their success depends on accurate knowledge of the dynamic behaviour of the machine. Additionally, passive control techniques have low versatility, i.e., any change in the machine configuration or in the loading condition may require a new damping device.

Viderman et al. and Subbiah et al. and [14-15] analyzed that a rotor has certain speed ranges in which large and unacceptable amplitude of vibration could be developed. These speed ranges are known as critical speeds (or critical frequencies) which could cause a bearing failure or result in excessive rotor deflection. Under these circumstances, the problem of ensuring that a rotor bearing system performs with stable and low-level amplitude of vibration becomes increasingly important. Dutt J.K. et al. [16] presented a viscoelastic support characteristics so that the frequency of excitation never coincides with any of the un damped natural frequencies of the system, thus giving low unbalance response over a wide frequency range and the support material can be chosen accordingly. Chen and Wang [17] presented an analysis and design of rotor-bearing systems with gyroscopic effects. They transformed the original problem of a damped system into state space form so that the transformed problem is similar to the eigenvalue problem of an undamped system. The problem is then solved by available eigenvalue solvers and the sensitivities needed for optimization were obtained. They used sequential linear programming to solve the unique design optimization problem.

Childs D.W. et al. [18-19] presented that eigen values are in general complex, where the sign of the real part decides stability. Negative real part confirms asymptotic stability whereas a non-negative value indicates instability. So for a particular speed of rotation, the maximum real part of the system eigenvalues should be negative for the stable operation of the rotor at that speed. The lowest speed, at which the maximum real part of the eigenvalues becomes nonnegative, is known as the stability limit speed (SLS) of the rotor-shaft system.

2.3 Finite element modelling and vibration analysis of FRP composite shaft system

There are many authors have been developed Finite element modelling and vibration analysis of FRP composite shaft system as follows:-

M. Y. Chang et al. [20] developed the vibration behaviors of rotating laminated composite shaft model where transverse shear deformation, rotary inertia, gyroscopic effects and coupling effect are incorporated. Bert developed governing equation of composite shaft, including effect of gyroscopic, bending and torsion coupling and determines critical speeds of composite shaft. Zinberg and Symmonds [21] analyzed a boron/epoxy composite tail rotor driveshaft for a helicopter. Equivalent modulus beam theory (EMBT) is used for evaluation of the critical speeds. Shaft is assumed thin walled circular tube simply supported at the ends. Shear deformation was not taken into consideration. Dos Reis et al. [22] developed an analytical analysis on thin-walled layered composite cylindrical hollow shaft. The beam element was extended to formulate the problem of a rotor supported on general eight coefficient bearings. Results were obtained for shaft configuration of Zinberg and Symmonds. The authors have shown that bending-stretching coupling and shear-normal coupling effects change with stacking sequence, and alter the frequency values. Gupta and Singh [23] studied the effect of shear-normal coupling on rotor natural frequencies and modal damping. Kim and Bert [24] have formulated the problem of determination of critical speeds of a composite shaft including the effects of bending-twisting coupling. The shaft was modeled as a Bresse-Timoshenko beam. The shaft gyroscopic has also been included. In another study, Bert and Kim [25] have analyzed the dynamic instability of a composite drive shaft subjected to fluctuating torque and/or rotational speed by using various thin shell theories. The rotational effects include centrifugal and Coriolis forces. Dynamic instability regions for a long span simply supported shaft are presented.

C. Y. Chang et al. [26] published the vibration analysis of rotating composite shafts containing randomly oriented reinforcements. The Mori-Tanaka mean-field theory is adopted here to account for the interaction at the finite concentrations of reinforcements in the composite material.

Pilkey et al [27] analyzed that Existence of support properties corresponding to optimum dynamic performance was also reported. Out of many works on predicting the optimum support properties an interesting one is by where the authors used the ‘‘linear programming technique’’ to predict the optimum support characteristics. Damping is a mechanism to dissipate mechanical energy in the form of heat. Muszynska [28] developed the paper which states that Unbalance is a most common malfunction in rotating machines. Unbalance in the rotating machine is a condition of unequal mass distribution at each section of the rotor. In an unbalanced condition, the rotor mass center line does not coincide with the axis of rotation. During rotation, rotor unbalance generates an inertia centrifugal force which rotates at the rotor rotational frequency. Unbalance represents then the first, fundamental mechanism to transfer the rotational energy into vibrations. Wettergren H. L. et al. [29] analyzed for a rotor system with viscous form of internal damping, stability limit is not expected until the first critical speed is reached. Instability can be postponed by introducing external damping and using right combination of non-isotropic bearing stiffness and damping coefficients along with some other factors.

Lananne and Ferraris [30] developed a finite element model of a multi-disc viscoelastic rotor with bearings. The model was based on Euler-Bernoulli beam theory. The study was based on a rotor with three discs with viscoelastic supports (Voigt Model) at both ends. The internal damping of the material of the rotor was taken into consideration. Finite

element model lead to Campbell Diagrams and Decay rate plot. These plots were used to show the stability characteristics of the system. DOI [31] developed the dynamic response of the considered mechanical system can be modelled by using variational mechanics equations as based on the Hamilton`s principle. For this aim, the strain energy of the shaft and the kinetic energies of the shaft and discs are calculated. An extension of Hamilton`s principle makes possible to include the effect of energy dissipation. The parameters of the bearings are considered in the model by using the principle of the virtual work.

Gustavsson [32] DeLaval and Jeffcott's names are still in use as the name of the simplified rotor model with the disc in the mid-span of the shaft. Jeffcott's rotor is described by Vance (1988), for example as one that consists of a flexible shaft, with zero mass, supported at its ends. The supports are rigid and allow rotation around the centre axis of the shaft. The mass is concentrated in a disk, fixed at the midpoint of the shaft. The system is geometrically symmetrical with respect to its rotational axis, except for a mass imbalance attached to the disk. When rotating the mass imbalance provides excitation to the system.
Nighil, et al. [33] analyzed that the magnetic force developed on the rotor by one pair of poles of the electromagnet is dealt with in details; However, salient portions are given here in brief for completeness, continuity and ease of understanding. Chang-Jian et al. [34] presented in a rotor-bearing system, the hydrodynamic pressure in journal bearings is generated entirely by the motion of the journal and depends on the viscosity of the lubricating fluid. However, the hydrodynamic pressure around the bearing is nonlinear and hence the fluid film rotor-bearing system has a strong nonlinearity which can cause substantial vibrations of the rotor and its bearings. Bueno [35] developed an increase of research works in engineering dedicated to the development of active vibration control techniques (AVC) is observed. This effort is stimulated by the necessity of lighter structures associated to higher operational performance and smaller operating costs. Das A.S. et al. [36] developed an arrangement of actuator poles is intended to apply non-contact type control force on the rotor-shaft over an air-gap that can be resolved into two orthogonal components along *Y*- and *Z*-directions, which can be computed independent of one another. Details of derivation of the expressions of linearized force components generated by the actuator with necessary assumptions are discussed. The components of the linearized control force obtained from the actuator in terms of control current and the displacement of the rotor-shaft at the location of the actuator of the controller.

Das A.S. et al. [37] analyzed that Rotor vibrations caused by large time-varying base motion are of considerable importance as there are a good number of rotors, e.g., the ship and aircraft turbine rotors, which are often subject to excitations, as the rotor base, i.e. the vehicle, undergoes large time varying linear and angular displacements as a result of different maneuvers. Due to such motions of the base, the equations of vibratory motion of a flexible rotor–shaft relative to the base (which forms a non-inertial reference frame) contains terms due to Coriolis effect as well as inertial excitations (generally asynchronous to rotor spin) generated by different system parameters. The actuator does not levitate the rotor or facilitate any bearing action, which is provided by the conventional suspension system. The equations of motion of the rotor–shaft continuum are first written with respect to the non-inertial reference frame (the moving base in this case) including the effect of rotor internal damping. A conventional model for the electromagnetic exciter is used.

Numerical simulations performed on the flexible rotor–shaft modelled using beam finite elements shows that the control action is successful in avoiding the parametric instability, postponing the instability due to internal material damping and reducing the rotor response relative to the rigid base significantly, with sufficiently low demand of control current in comparison with the bias current in the actuator coils. In the rotor dynamics applications elastic behaviour of a rotating shaft is an important concern. There are several works in the literature on the modelling and vibration control of a flexible shaft since the analysis of flexible structure with lumped parameters does not reflects the real behaviour, continuous time models with partial differential equations are used for more realistic analysis. The well known classical beam theory also called as Euler-Bernoulli beam theory has been used by many authors for the vibration analysis of the shafts. However, this beam theory is not suitable for thick beams since the shear deformation and rotary inertia effects are not included in the model.

2.4 Active vibration control of rotor shaft system

There are various methods have been adopted by many researchers to control active vibration.

Schweitzer et al. et al. [38-39] developed an active magnetic bearings (AMB) provide an active way of bearing action and vibration control over an air gap which is more elegant. That measures the unbalance force with the help of sensor and applies the control force between the outer race and the bearing housing. Schittenhelm et al [40] developed a linear quadratic regulator is designed for a rotor system on the basis of a finite element model. The rotor is subject to gyroscopic effect and is actively supported by means of piezoelectric actuators installed at one of its two bearings. As a result of the first aspect, its dynamic behavior varies with rotational frequency of the rotor. This aspect is challenging for linear time invariant control techniques since it results in a demand for high robustness. Furthermore, if controller and observer are calculated using a model at a specific design frequency, the separation principle does not hold. In this article a proposal for combined Linear Quadratic Regulator and Kalman Filter design on the basis of physical considerations is given. Maslen [41] presented an Active Magnetic Bearings (AMB) not only as a main support bearing in a machine but also as force actuators has become one of the useful devices in a control scheme for active vibration control in rotating machinery such as suspension systems for shafts or rotors. Several components of an AMB are characterized by nonlinear behavior and therefore the entire system is inherently nonlinear.

Many methods have been proposed to reduce the unbalance-induced vibration, where different devices such as electromagnetic bearings, active squeeze film dampers, lateral force actuators, active balancers and pressurized bearings have been developed by Blanco et al. [42], Guozhi et al. [43], Jinhao & Kwon, [44], Palazzolo et al. [45], Sheu et al. [46], Zhou & Shi [47]. Passive and active balancing techniques are based on the unbalance estimation to attenuate the unbalance response in the rotating machinery. The Influence Coefficient Method has been used to estimate the unbalance while the rotating speed of the rotor is constant presented by Lee et al. [48], Yu [49]. This method has been used to estimate the unknown dynamics and rotor- bearing system unbalance during the speed-varying period Zhou et al. [50]. On the other hand, there is a vast literature on identification methods developed by

Ljung [51], Sagara & Zhao [52] , Sagara & Zhao [53] which are essentially asymptotic, recursive or complex, which generally suffer of poor speed performance.

Lund J. [54] analyzed vibrations are of two types, active and passive vibration and both passive and active means of vibration minimization techniques are reported in literature; these techniques attempt to find suitable stiffness-damping combinations of the support to avoid or minimize resonant response. The passive category includes the use of flexible–damped supports, Squeeze-film dampers and viscoelastic bearing supports. The measures require contact with the support element for its mechanical deflection to get the control force and are applied for convenience between the bearing outer-race and the bearing housing.

Allaire et al. [55] developed and presented magnetic bearings in a multimass flexible rotor both as support bearings and as vibration controller and demonstrated the beneficial effect of reducing vibration amplitudes by using an electromagnet applied to a transmission shaft respectively. They used two approaches to actively control flexible rotors. In the first approach magnetic bearings or electromagnetic actuators are used to apply control forces directly to the rotating rotor without contacting it. In the second approach, the control forces of the electro-magnetic actuators are applied to the bearing housings.

Koroishi E. H. et al. [56] presented a paper proposes a simple model of an electromagnetic actuator (EMA) for active vibration control (AVC) of rotor systems. For this purpose, the actuator was linearized by adopting a behavior that is similar to the one used for active magnetic bearings (AMB). The results show the validity of the proposed model and the effectiveness of the control. Koroishi [57] developed In recent years, a number of new methods dedicated to acoustic and vibration attenuation have been developed and proposed aiming at handling several types of engineering problems related to the dynamic behavior of the system. This is mainly due to the demand for better performance and safer operation of mechanical systems. There are various types of actuators available. The present contribution is dedicated to the electromagnetic actuator (EMA). EMA uses electromagnetic forces to support the rotor without mechanical contact.

Keith et al. [58] analyzed that the use of electromagnetic bearings in lowering the amplitude level has increased and) showed that they generate no mechanical loss and need no lubricants such as oil or air as they support the rotor without physical contact. Cheung et al. [59] presented the electromagnets are open loop unstable and all designs require external electronic control to regulate the forces acting on the bearing. Abduljabbar et al. [60] developed an optimal controller based on characteristics peculiar to rotor bearing systems which take into account the requirements for the free vibration and the persistent unbalance excitations. The controller uses as feedback signals, the states and the unbalance forces. A methodology of selecting the gains on the feedback signals has been presented based on separation of the signal effects: the plant states are the primary stimuli for stabilizing the rotor motion and augmenting system damping, while the augmented states representing the unbalance forces are the primary stimuli for counteracting the periodically excited vibration. The results demonstrate that the proposed controller can significantly improve the dynamical behaviour of the rotor-bearing systems with regard to resonance and instabilities. A passive vibration control devices are of limited use. This limitation together with the desire to exercise greater control over rotor vibration, with greatly enhanced performance, has led to a growing interest in the development of active control of rotor vibrations.

ROY T. et al [61] analyzed that the linear quadratic regulator (LQR) control approach has been found to be effective in vibration control with appropriate weighting matrices, which gives optimal control gain by minimizing the performance index. The weighting matrices [Q] and [R] are the most important components in LQR optimization .The combinations of [Q] and [R] matrices greatly affect the output performance and input cost of the system and hence an optimal selection of these weighting matrices is of significant importance from the control point of view. Serdar Cole M.O.T. et al [62] developed that the use of an Active Magnetic Bearing (AMB) to attenuate the lateral vibration of a rotor under simultaneous excitations from mass unbalance and an initial base impact, which is quasi-stationary in nature. For the implementation and testing of the devised multi frequency vibration control strategy, a flexible rotor facility was used. Multi frequency feedback control was implemented in order to control rotor vibration at the synchronous frequency and the first two harmonics.

Jingjun Zhang et al. [63] analyzed that the transfer function is transformed to a state space vector dynamic equation for state feedback control system design. To minimize the displacement of the rotor shaft system, the Linear Quadratic Regulator (LQR) based on independent mode space control techniques is designed. The control voltage for the actuators is determined by the optimal control solution of the Linear Quadratic Regulator (LQR), which is an effective and widely used linear control technique. Provided the full state vector is observable, this method can be employed to meet specific design and performance criteria. A quadratic cost function is used to minimize the performance index. The recent years have seen the appearance of innovative systems for acoustic and vibration attenuation, most of actuators them integrating new actuator technologies. In this sense, the study of algorithms for active vibrations control in rotating machinery became an area of enormous interest, mainly due to the countless demands of an optimal performance of mechanical systems in aircraft automotive structures. Also, many critical machines such as compressors, pumps and gas turbines continue to be used beyond ft, aerospace and automotive structures. Also, many critical machines such as compressors, pumps and gas turbines continue to be used beyond their expected service life despite the associated potential for failure due to damage accumulation.

Koroishi, et al. [64] presented that the AMB is a feedback mechanism that supports a spinning shaft by levitating it in a magnetic field. For its operation, the sensor measures the relative position of the shaft and the measured signal is sent to the controller where it is processed. Then, the signal is amplified and fed as electric current into the coils of the magnet, generating an electromagnetic field that keeps the shaft in a desired position. The strength of the magnetic field depends both on the air gap between the shaft and the magnet and the dynamics of the system including the design

Janik et al. [65] analyzed that In order to invoke control force for reducing the amplitude of rotor vibration an electromagnetic actuator is used which is capable of applying non-contact type force of actuation over an air-gap on the rotor-shaft. The actuator consists of four exciters (each having a pair of electromagnetic poles) symmetrically arranged within a stator casing around the periphery of the rotor section. This actuator system can be placed at any suitable location along the span of the rotor-shaft avoiding the bearing as well as disc locations. Dutt and Toi [66] presented a Polymeric material in the form of sectors has been considered in this work as bearing supports. Polymeric material has been considered in this

work as both stiffness and loss factor of such materials varies with the frequency of excitation. Stiffness and loss factor have been found out for the proposed support system comprising of polymeric sectors.

Meirovitch, L. [67] presents mathematical modeling and numerically verified using the feedback pole allocation control. The goal of linear feedback control is to place the closed loop poles on the left half of the complex plane of the eigen values, so as to ensure asymptotic stability of the closed loop system. One approach consists of prescribing first the closed-loop poles associated with the modes to be controlled and then computing the control gains required to produce these poles. Because this amounts to controlling a system by controlling its modes, this approach is known as modal control.

In this way, this paper presents a developed approach for active vibration control in a rotor using Active Magnetic Bearings (AMB) that is numerically verified. The feedback technique is used for this controlling device and the controller gain is obtained by the pole allocation. The AMB uses electromagnetic forces to support a rotor without mechanical contact. It offers many advantages compared to fluid film and rolling element bearings, such as no wear, the ability to operate in high temperature environments, and no contamination of the working fluid due to the absence of lubricant in the system.

2.5 Motivation and Objectives of the present work

Based on the literature review it has been observed that many works have been carried out for the modelling analysis of rotor shaft system using finite element method. In the direction of composite rotor shaft system few works are also available. The use of composite material is increasing day by day in the various industries because of FRP composites are lighter, more durable and have infinite design flexibility. So details study of laminated composite shaft is required. Due to its light weight and flexibility this types of shafts do not sustains large vibration in the operational condition. Active vibration control of rotating composite shaft is also very important in the area of research. Therefore the objectives of the present works are laid down as follows:

- Finite element modelling for vibration analysis for rotating composite shaft, with disk and bearing.
- Effect of ply angle on the responses of the composite shaft.
- Modelling of electromagnetic actuator and
- Study of active vibration control of rotating composite shaft using electromagnetic actuators and PD control scheme.

CHAPTER 3

FINITE ELEMENT MODELLING AND ANALYSIS OF FRP COMPOSITE SHAFT SYSTEM

3.1 Introduction

The composite-material shafts have been sought as new potential subject for replacement of the conventional metallic shafts in many application areas. This may be attributed to the improved performance of the shaft system resulting from the use of the composite materials. It was in fact demonstrated by Faust et al.via testing the composite transmission shafts of twin-propeller helicopters that the composite shaft not only is lighter in weight and has a lower vibration level, but also has greater strength and a longer service life compared with its metallic counterparts. Accompanied by the development of many new advanced composite materials, various mathematical models of spinning composite shafts were also developed by researchers. Zinberg and Symonds who used an equivalent modulus beam theory (EMBT) to model the composite shaft and compared the critical speeds with those of the tests they had performed. dos Reis et al. incorporated the Timoshenko beam theory with the Donnell thin shell theory to derive the stiffness matrix of rotating composite shafts. They then adopted the approximate finite element approach of Ruhl and Booker to derive the equations of motion of systems. The model was used to analyze the critical speeds of thin-walled composite shafts developed [20].

The shaft is modelled as a Timoshenko beam with rotary inertia and gyroscopic effect is used. The shaft rotates at constant speed about its longitudinal axis the shaft has a uniform, circular cross-section.

3.2 Mathematical Modelling of composite Rotor shaft system

To derive the strain energy expression of the composite shaft, the following form of the displacement fields of the shaft are assumed.

$$u_x(x,\ y,\ z,\ t) = u(x,t) + z\beta_x(x,t) - y\beta_y(x,t) \tag{3.1}$$

$$u_y(x,\ y,\ z,\ t) = v(x,t) - z\phi(x,t)$$

$$u_z(x,\ y,\ z,\ t) = w(x,t) + y\phi(x,t)$$

The stress-strain relations of the i^{th} layer expressed in the cylindrical coordinate system can be expressed as:

$$\sigma_{xx} = \bar{Q}_{11i}\varepsilon_{xx} + k_s\bar{Q}_{16i}\gamma_{x\theta} \tag{3.2}$$

$$\tau_{x\theta} = k_s Q_{16i}\varepsilon_{xx} + k_s Q_{66i}\gamma_{x\theta}$$

$$\tau_{xr} = k_s\bar{Q}_{55i}\gamma_{xr}$$

Where, k_s is the shear correction factor, $\overline{Q}_{ijn}$ is the constitutive matrix which is related to lamination angle η and elastic constants of principle axes.

Where,

$$A_{11} = \pi\sum_{i=1}^{n}\overline{Q}_{11i}(r_{i+1}^2 - r_i^2)$$

$$A_{55} = \frac{\pi}{2}\sum_{i=1}^{n}\overline{Q}_{55i}(r_{i+1}^2 - r_i^2)$$

$$A_{66} = \frac{\pi}{2}\sum_{i=1}^{n}\overline{Q}_{66i}(r_{i+1}^2 - r_i^2)$$

$$B_{16} = \frac{2\pi}{3}\sum_{i=1}^{n}\overline{Q}_{16i}(r_{i+1}^3 - r_i^3)$$

$$D_{11} = \frac{\pi}{4}\sum_{i=1}^{n}\overline{Q}_{11i}(r_{i+1}^4 - r_i^4)$$

$$D_{66} = \frac{\pi}{2}\sum_{i=1}^{n}\overline{Q}_{66i}(r_{i+1}^4 - r_i^4)$$

3.2 Finite element model analysis of rotor shaft

The equation of motion of the composite rotor-shaft-bearing system has been derived using the finite element method and the rotor-shaft has also been modeled and analyzed Timoshenko beam theory by three nodded element beams, each node having 4 degree of freedom. The governing equations of the motion are expressed below as ordinary differential equations:

$$[M]\{\ddot{q}\} + ([C] + \Omega[G])\{\dot{q}\} + [K]\{q\} = \{F\} \tag{3.3}$$

Where $[M]$ denotes the mass matrix, $[G]$ denotes the gyroscopic matrix, $[C]$ denotes the total damping matrix which include the material internal damping, bearing damping and

actuator damping, $[K]$ denotes the stiffness matrix , $\{q\}$ denotes the displacement vector, $\{F\}$ represents the external force vector.

Mass matrices

To find out mass matrices assumes that field variable velocity is represents as, $\dot{v}_0 = \sum_{i=1}^{n} \psi_n(x)\dot{v}_{0n}$

Now, kinetic energy expression $T = \frac{1}{2}\int_0^L \rho A\left\{\dot{v}_0\right\}^2 dx = \frac{1}{2}\rho A\int_0^L \left\{\sum_{i=1}^{n}\psi_n(x)\dot{v}_{0n}\right\}^2 dx$

So, mass matrices for an element

$$M_{ij} = \frac{\partial}{\partial v_{0i}}\frac{\partial}{\partial v_{0j}}\frac{1}{2}\rho A\int_0^L \left\{\sum_{j=1}^{n}\sum_{i=1}^{n}\psi_n(x)\dot{v}_{0n}\right\}^2 dx = \int_0^L \rho A\psi_{ni}(x)\psi_{nj}(x)dx$$

$$[M_e] = \begin{bmatrix} [M_{22}]_{3\times3} & 0 & 0 & 0 \\ 0 & [M_{33}]_{3\times3} & 0 & 0 \\ 0 & 0 & [M_{44}]_{3\times3} & 0 \\ 0 & 0 & 0 & [M_{55}]_{3\times3} \end{bmatrix}_{12\times12}$$

$$M_{22}^{ij} = \int_0^L I_m\psi_i(x)\psi_j(x)dx + \int_0^L \sum_{i=1}^{N_D} \mathrm{I}_m^D\psi_i(x)\psi_j(x)\Delta\left(x - x_{Di}\right)dx$$

$$M_{33}^{ij} = \int_0^l I_m\psi_i(x)\psi_j(x)dx + \int_0^l \sum_{i=1}^{N_D} \mathrm{I}_m^D\psi_i(x)\psi_j(x)\Delta\left(x - x_{Di}\right)dx$$

$$M_{44}^{ij} = \int_0^l I_d\psi_i(x)\psi_j(x)dx + \int_0^l \sum_{i=1}^{N_D} \mathrm{I}_d^D\psi_i(x)\psi_j(x)\Delta\left(x - x_{Di}\right)dx$$

$$M_{55}^{ij} = \int_0^l I_d\psi_i(x)\psi_j(x)dx + \int_0^l \sum_{i=1}^{N_D} \mathrm{I}_d^D\psi_i(x)\psi_j(x)\Delta\left(x - x_{Di}\right)dx$$

Stiffness Matrix

Now stiffness matrix expression $K = \int_V [B]^T[D][B]dV$

Now from the following relation $\left[\frac{\partial}{\partial x}\right] = \left[\frac{\partial}{\partial \eta}\right]\left[\frac{\partial \eta}{\partial x}\right] = \left[\frac{\partial x}{\partial \eta}\right]^{-1}\left[\frac{\partial}{\partial \eta}\right] = J^{-1}\left[\frac{\partial}{\partial \eta}\right]$

Where $J^{-1} = \left[\frac{\partial x}{\partial \eta}\right]^{-1}$

$$\frac{\partial v_0}{\partial \eta} = \frac{\partial}{\partial \eta}(\psi_1 v_{01} + \psi_2 v_{02} + \psi_3 v_{03}) = (\psi'_1 v_{01} + \psi'_2 v_{02} + \psi'_3 v_{03})$$

$$\frac{\partial v_{0i}}{\partial \eta} = [\psi'_i]\{v_{0i}\}$$

Now following

$$B = \begin{bmatrix} 0 & 0 & r\sin\theta J^{-1}\psi' & -r\cos\theta J^{-1}\psi' \\ -\sin\theta J^{-1}\psi' & \cos\theta J^{-1}\psi' & \cos\theta & \sin\theta \\ \cos\theta J^{-1}\psi' & \sin\theta J^{-1}\psi' & \sin\theta & -\cos\theta \end{bmatrix}$$

Now following $[B]^T[D][B] =$

$$\begin{bmatrix} -k_s\bar{C}_{16}\sin\theta J^{-1}\psi' & -k_s\bar{C}_{66}\sin\theta J^{-1}\psi' & k_s\bar{C}_{55}\cos\theta J^{-1}\psi' \\ k_s\bar{C}_{16}\cos\theta J^{-1}\psi' & k_s\bar{C}_{66}\cos\theta J^{-1}\psi' & k_s\bar{C}_{55}\sin\theta J^{-1}\psi' \\ \bar{C}_{11}r\sin\theta J^{-1}\psi' + k_s\bar{C}_{16}\cos\theta & k_s\bar{C}_{16}r\sin\theta J^{-1}\psi' + k_s\bar{C}_{66}\cos\theta & k_s\bar{C}_{55}\sin\theta \\ -\bar{C}_{11}r\cos\theta J^{-1}\psi' + k_s\bar{C}_{16}\sin\theta & -k_s\bar{C}_{16}r\cos\theta J^{-1}\psi' + k_s\bar{C}_{66}\sin\theta & -k_s\bar{C}_{55}\cos\theta \end{bmatrix} \times$$

$$\begin{bmatrix} 0 & 0 & r\sin\theta J^{-1}\psi' & -r\cos\theta J^{-1}\psi' \\ -\sin\theta J^{-1}\psi' & \cos\theta J^{-1}\psi' & \cos\theta & \sin\theta \\ \cos\theta J^{-1}\psi' & \sin\theta J^{-1}\psi' & \sin\theta & -\cos\theta \end{bmatrix}$$

After matrix operation and simplifications, obtains

$$[K] = \begin{bmatrix} [K_{22}]_{3\times3} & [K_{23}]_{3\times3} & [K_{24}]_{3\times3} & [K_{25}]_{3\times3} \\ [K_{32}]_{3\times3} & [K_{33}]_{3\times3} & [K_{34}]_{3\times3} & [K_{35}]_{3\times3} \\ [K_{42}]_{3\times3} & [K_{43}]_{3\times3} & [K_{44}]_{3\times3} & [K_{45}]_{3\times3} \\ [K_{52}]_{3\times3} & [K_{53}]_{3\times3} & [K_{54}]_{3\times3} & [K_{55}]_{3\times3} \end{bmatrix}_{12\times12}$$

$$K_{22}^{ij} = \int_0^r \int_0^{2\pi} \int_0^l \left\{ k_s (J^{-1}\psi')^2 (\bar{C}_{66}\sin^2\theta + \bar{C}_{55}\cos^2\theta) + \sum_{i=1}^{N_B} K_{yy}^{Bi}\Delta(x - x_{Bi}) \right\} r.d\theta dx dr$$

$$= \int_0^l \left\{ k_s \left(A_{55} + A_{66}\right) \frac{\partial \psi_i}{\partial x}\frac{\partial \psi_j}{\partial x} + \sum_{i=1}^{N_B} K_{yy}^{Bi}\psi_i\psi_j\Delta(x - x_{Bi}) \right\} dx$$

$$K_{23}^{ij} = \int_0^r \int_0^{2\pi} \int_0^l \left\{ k_s (J^{-1}\psi')^2 \sin\theta\cos\theta(-\bar{C}_{66} + \bar{C}_{55}) + \sum_{i=1}^{N_B} K_{yz}^{Bi}\Delta(x - x_{Bi}) \right\} r.d\theta.dx.dr$$

$$= \int_0^l \sum_{i=1}^{N_B} K_{yz}^{Bi}\psi_i\psi_j\Delta(x - x_{Bi})dx$$

$$K_{24}^{ij} = \int_0^r \int_0^{2\pi} \int_0^l \left\{ k_s (J^{-1}\psi')(-\bar{C}_{16}r\sin^2\theta J^{-1}\psi' - \bar{C}_{66}\sin\theta\cos\theta + \bar{C}_{55}\sin\theta\cos\theta) \right\} r.d\theta.dx.dr$$

$$= \int_0^l -\frac{1}{2}K_s A_{16}\frac{\partial \psi_i}{\partial x}\frac{\partial \psi_j}{\partial x}dx$$

$$K_{25}^{ij} = \int_0^r \int_0^{2\pi} \int_0^l \left\{ k_s (J^{-1}\psi')(\overline{C}_{16} r \sin\theta \cos\theta J^{-1}\psi' - \overline{C}_{66} \sin^2\theta - \overline{C}_{55} \cos^2\theta) \right\} r.d\theta.dx.dr$$

$$= \int_0^l -K_s (A_{55} + A_{66}) \frac{\partial \psi_i}{\partial x} \psi_j dx$$

$$K_{32}^{ij} = \int_0^r \int_0^{2\pi} \int_0^l \left\{ k_s (J^{-1}\psi')^2 \sin\theta \cos\theta (-\overline{C}_{66} + \overline{C}_{55}) + \sum_{i=1}^{N_B} K_{yz}^{Bi} \Delta(x - x_{Bi}) \right\} r.d\theta.dx.dr$$

$$= \int_0^l \sum_{i=1}^{N_B} K_{yz}^{Bi} \psi_i \psi_j \Delta(x - x_{Bi}) dx$$

$$K_{33}^{ij} = \int_0^r \int_0^{2\pi} \int_0^l \left\{ k_s (J^{-1}\psi')^2 (\overline{C}_{55} \sin^2\theta + \overline{C}_{66} \cos^2\theta) + \sum_{i=1}^{N_B} K_{zz}^{Bi} \Delta(x - x_{Bi}) \right\} r.d\theta dx dr$$

$$= \int_0^l \left\{ k_s \left(A_{55} + A_{66} \right) \frac{\partial \psi_i}{\partial x} \frac{\partial \psi_j}{\partial x} + \sum_{i=1}^{N_B} K_{zz}^{Bi} \psi_i \psi_j \Delta(x - x_{Bi}) \right\} dx$$

$$K_{34}^{ij} = \int_0^r \int_0^{2\pi} \int_0^l \left\{ k_s (J^{-1}\psi')(\overline{C}_{16} r \sin\theta \cos\theta J^{-1}\psi' + \overline{C}_{55} \sin^2\theta + \overline{C}_{66} \cos^2\theta) \right\} r.d\theta dx dr = \int_0^l k_s \left(A_{55} + A_{66} \right) \frac{\partial \psi_i}{\partial x} \psi_j dx$$

$$K_{35}^{ij} = \int_0^r \int_0^{2\pi} \int_0^l \left\{ k_s (J^{-1}\psi')(-\overline{C}_{16} r \cos^2\theta J^{-1}\psi' + \sin\theta \cos\theta (\overline{C}_{66} - \overline{C}_{55})) \right\} r.d\theta.dx.dr = \int_0^l -\frac{1}{2} k_s A_{16} \frac{\partial \psi_i}{\partial x} \frac{\partial \psi_j}{\partial x} dx$$

$$K_{42}^{ij} = \int_0^r \int_0^{2\pi} \int_0^l \left\{ k_s (J^{-1}\psi')(-\overline{C}_{16} r \sin^2\theta J^{-1}\psi' + \sin\theta \cos\theta (-\overline{C}_{66} + \overline{C}_{55})) \right\} r.d\theta.dx.dr = \int_0^l -\frac{1}{2} k_s A_{16} \frac{\partial \psi_i}{\partial x} \frac{\partial \psi_j}{\partial x} dx$$

$$K_{43}^{ij} = \int_0^r \int_0^{2\pi} \int_0^l \left\{ k_s (J^{-1}\psi')(\overline{C}_{16} r \sin\theta \cos\theta J^{-1}\psi' + \overline{C}_{55} \sin^2\theta + \overline{C}_{66} \cos^2\theta) \right\} r.d\theta dx dr = \int_0^l k_s \left(A_{55} + A_{66} \right) \frac{\partial \psi_i}{\partial x} \psi_j dx$$

$$K_{44}^{ij} = \int_0^r \int_0^{2\pi} \int_0^l \left\{ \begin{array}{l} (\overline{C}_{11} r^2 \sin^2\theta (J^{-1}\psi')^2 + 2k_s \overline{C}_{16} r \sin\theta \cos\theta (J^{-1}\psi') \\ + k_s \overline{C}_{66} \cos^2\theta + k_s \overline{C}_{55} \sin^2\theta) \end{array} \right\} r.d\theta.dx.dr$$

$$= \int_0^l \left\{ B_{11} \frac{\partial \psi_i}{\partial x} \frac{\partial \psi_j}{\partial x} + k_s \left(A_{55} + A_{66} \right) \psi_i \psi_j \right\} dx$$

$$K_{45}^{ij} = \int_0^r \int_0^{2\pi} \int_0^l \left\{ \begin{array}{l} (-\overline{C}_{11} r^2 \sin\theta \cos\theta (J^{-1}\psi')^2 - k_s \overline{C}_{16} r (J^{-1}\psi')(\cos^2\theta - \sin^2\theta) \\ + k_s \sin\theta \cos\theta (\overline{C}_{66} - \overline{C}_{55}) \end{array} \right\} r.d\theta.dx.dr$$

$$= \int_0^l \left\{ \frac{1}{2} k_s A_{16} \frac{\partial \psi_i}{\partial x} \psi_j - \frac{1}{2} k_s A_{16} \frac{\partial \psi_j}{\partial x} \psi_i \right\} dx$$

$$K_{52}^{ij} = \int_0^r \int_0^{2\pi} \int_0^l k_s (J^{-1}\psi')(\overline{C}_{16} r \sin\theta \cos\theta J^{-1}\psi' - \overline{C}_{66} \sin^2\theta - \overline{C}_{55} \cos^2\theta) r.d\theta.dx.dr$$

$$= \int_0^l -K_s (A_{55} + A_{66}) \frac{\partial \psi_i}{\partial x} \psi_j dx$$

$$K_{53}^{ij}=\int_0^r\int_0^{2\pi}\int_0^l\left\{k_s(J^{-1}\psi')(-\overline{C}_{16}r\cos^2\theta J^{-1}\psi'+\sin\theta\cos\theta(\overline{C}_{66}-\overline{C}_{55}))\right\}r.d\theta.dx.dr=\int_0^l-\frac{1}{2}k_sA_{16}\frac{\partial\psi_i}{\partial x}\frac{\partial\psi_j}{\partial x}dx$$

$$K_{54}^{ij}=\int_0^r\int_0^{2\pi}\int_0^l\begin{Bmatrix}(-\overline{C}_{11}r^2\sin\theta\cos\theta(J^{-1}\psi')^2+k_s\overline{C}_{16}r(J^{-1}\psi')(\sin^2\theta-\cos^2\theta)\\+k_s\sin\theta\cos\theta(\overline{C}_{66}-\overline{C}_{55})\end{Bmatrix}r.d\theta.dx.dr$$

$$=\int_0^l\left\{\frac{1}{2}k_sA_{16}\frac{\partial\psi_i}{\partial x}\psi_j-\frac{1}{2}k_sA_{16}\frac{\partial\psi_j}{\partial x}\psi_i\right\}dx$$

$$K_{55}^{ij}=\int_0^r\int_0^{2\pi}\int_0^l\begin{Bmatrix}(\overline{C}_{11}r^2\cos^2\theta(J^{-1}\psi')^2-2k_s\overline{C}_{16}rJ^{-1}\psi'\sin\theta\cos\theta\\+k_s\overline{C}_{66}\sin^2\theta+k_s\overline{C}_{55}\cos^2\theta\end{Bmatrix}r.d\theta.dx.dr$$

$$=\int_0^l\left\{B_{11}\frac{\partial\psi_i}{\partial x}\frac{\partial\psi_j}{\partial x}+k_s\left(A_{55}+A_{66}\right)\psi_i\psi_j\right\}dx$$

Damping Matrix of Bearing

$$\left[C_e^B\right]=\begin{bmatrix}[C_{22}]_{3\times3} & [C_{23}]_{3\times3} & [0]_{3\times3} & [0]_{3\times3}\\ [C_{32}]_{3\times3} & [C_{33}]_{3\times3} & [0]_{3\times3} & [0]_{3\times3}\\ [0]_{3\times3} & [0]_{3\times3} & [0]_{3\times3} & [0]_{3\times3}\\ [0]_{3\times3} & [0]_{3\times3} & [0]_{3\times3} & [0]_{3\times3}\end{bmatrix}_{12\times12}$$

Now, $$C_{22}^{ij}=\int_{x_i}^{x_f}\left\{\sum_{i=1}^{N_B}C_{yy}^{Bi}\psi_i\psi_j\Delta(x-x_{Bi})\right\}dx$$

$$C_{23}^{ij}=\int_{x_i}^{x_f}\left\{\sum_{i=1}^{N_B}C_{yz}^{Bi}\psi_i\psi_j\Delta(x-x_{Bi})\right\}dx$$

$$C_{32}^{ij}=\int_{x_i}^{x_f}\left\{\sum_{i=1}^{N_B}C_{zy}^{Bi}\psi_i\psi_j\Delta(x-x_{Bi})\right\}dx$$

$$C_{33}^{ij}=\int_{x_i}^{x_f}\left\{\sum_{i=1}^{N_B}C_{zz}^{Bi}\psi_i\psi_j\Delta(x-x_{Bi})\right\}dx$$

Gyroscopic Matrix

$$\left[G_e\right]=\begin{bmatrix}[0]_{3\times3} & [0]_{3\times3} & [0]_{3\times3} & [0]_{3\times3}\\ [0]_{3\times3} & [0]_{3\times3} & [0]_{3\times3} & [0]_{3\times3}\\ [0]_{3\times3} & [0]_{3\times3} & [0]_{3\times3} & [G_{45}]_{3\times3}\\ [0]_{3\times3} & [0]_{3\times3} & [G_{54}]_{3\times3} & [0]_{3\times3}\end{bmatrix}_{12\times12}$$

In which

$$[G_{45}]_{3\times3} = \int_{x_i}^{x_f} I_P \psi_i \psi_j dx + \int_{x_i}^{x_f} \sum_{i=1}^{N_D} I_P^D \psi_i \psi_j \Delta(x - x_{Di}) dx$$

$$[G_{54}]_{3\times3} = \int_{x_i}^{x_f} -I_P \psi_i \psi_j dx + \int_{x_i}^{x_f} \sum_{i=1}^{N_D} -I_P^D \psi_i \psi_j \Delta(x - x_{Di}) dx$$

Displacement Vector

$$\{q_e\} = \left\{ \{v_e\}^T \{w_e\}^T \{\beta_{xe}\}^T \{\beta_{ye}\}^T \right\}_{1\times12}$$

Force Vector

$$\{F^e\} = \left\{ \{R_y^e\}^T \{R_z^e\}^T \{M_x^e\}^T \{M_y^e\}^T \right\}_{1\times12}$$

CHAPTER 4

MODELLING OF ELECTROMAGNETIC ACTUATOR

4.1 Introduction

In principle, the actuator consists of a current driven coil placed between two permanent magnets. Repellent forces are generated between the coil and the magnets, centering the coil between the two magnets. The 2D finite element analyses are carried out to predict the forces generated by this arrangement depending on coil current and coil position. Force measurements are also made using the actual device.

Actuator forces as predicted by the finite element analyses are in excellent agreement with the measured data, confirming the validity of the numerical model. Stiffness of the actuator is defined as the increase of force per unit of coil displacement. Actuator stiffness depends linearly on the coil current but in a nonlinear manner on the coil displacement. The performance of the actuator is sufficient to demonstrate the effect of a so-called parametric anti-resonance on a test stand.

4.2 The Electromagnetic Force

The magnetic force developed on the rotor by one pair of poles of the electromagnet. The corresponding centres of the shaft at its nominal or reference position (when the shaft is not vibrating) and the deflected position are OB and OC respectively. Assuming that (1) radial air gap between rotor and stator poles is insignificant compared to the rotor radius *R* and there is no fringing effect of magnetic flux lines near the pole-face, (2) flux leakage is negligible, (3) all individual magnetic flux lines have equal length, (4) magnetic materials obey linear relationship between flux density (*B*) and the magnetic-field-intensity (*H*) within the material, μ_i being the magnetic permeability [36].

$$F_{mag}(t) = -k_M * \frac{i(t)^2}{l_g^{\,2}} \tag{4.1}$$

Where,

$$k_M = \frac{\mu_0 A_p N^2}{4} \tag{4.2}$$

μ_0, A_P, and N are the absolute permeability of free air, pole face area, and number of coil turns respectively. The negative sign indicates that electromagnetic force increases with decrease in air gap. For nominal position of the rotor, uniform air gap g_o exists between the poles and the rotor surface and a steady bias current of magnitude i_o passes through all the coils of the exciters. Consequently the rotor is attracted equally by all the pairs of poles. At any given instant during the vibration of the rotor, it comes closer to a particular pair of poles, and goes

further from the opposite pair. The control force to oppose deflection of the shaft along any direction (either *Y* or *Z*) is achieved by simultaneously stepping up the current in the coil around the particular pair of poles, from which the rotor is farther, and stepping down the current in the coil around the opposite pair, to which the rotor is nearer, by equal amount from the steady bias current. The amount by which the current is stepped up or stepped down is called the control current. The geometry has the advantage that the forces in the *Y* and *Z* directions are (almost) uncoupled and can be calculated separately [36].

$$F_{Ymag} = k_{mag}\left\{\left(\frac{i_0 + i_{cY}}{g_0 + y}\right)^2 - \left(\frac{i_0 - i_{cY}}{g_0 - y}\right)^2\right\} \tag{4.3}$$

$$F_{Zmag} = k_{mag}\left\{\left(\frac{i_0 + i_{cZ}}{g_0 + z}\right)^2 - \left(\frac{i_0 - i_{cZ}}{g_0 - z}\right)^2\right\} \tag{4.4}$$

Due to an included angle of 2α between the poles, the magnetic exciter constant is:

$$k_{mag} = k_M \cos(\alpha)$$

4.2.1 Linearization of the Electromagnetic Force about operating Point

Above eg.(4) & eg.(5) are nonlinear relation of magnetic force. So we have to linearize around an operating point. Let displacement $Y=Y_{OP}$ and $Z=Z_{OP}$ and control current $i_{cY}= i_{Cyop}$ and $i_{cZ}= i_{cZOP}$ along *Y* and *Z* directions [36]. Linearized expression of forces F_Y and F_Z about an operating point can be written as:

$$F_Y = k_i i_{cY} + k_Y v \tag{4.5}$$

$$F_Z = k_i i_{cZ} + k_Z w \tag{4.6}$$

Where, $k_i = 4k_{mag}\frac{i_0}{g_0^2}$; $k_v = k_Z = k_S = -4k_{mag}\frac{i_0^2}{g_0^3}$

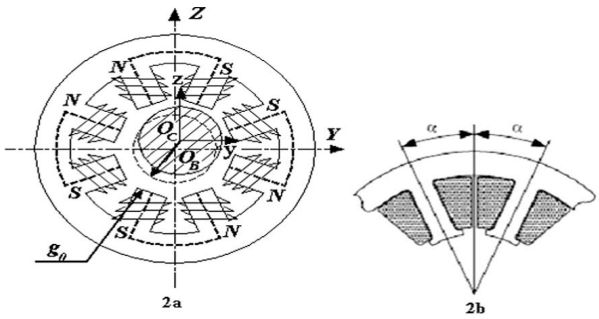

Fig.4.1: (a) Stator configuration of actuator; (b) Arrangement of coils and poles of the electromagnetic actuator [36]

4.3 Governing equation of motion

Equations of motion of a general multiple-disc flexible rotor shaft- bearing system is developed using finite element discretization technique. The flexible rotor shaft is modelled with three-nodded Rayleigh beam finite with distributed inertia and stiffness properties. Rotor discs are mounted on rotor-shaft and modelled as rigid, concentrated inertia elements. The bearing is supposed to offer supporting forces to the rotor-shaft system which is considered to be acting at a single node at the location of the bearing. The bearing forces are expressed in terms of four stiffness and four damping coefficients associated with that particular bearing. Equations of motion of such a rotor-shaft bearing system can be expressed as:

$$[M]\{\ddot{q}\} + [D]\{\dot{q}\} + [K]\{q\} = \{f\} + \{f_{EMA}\} \quad (4.7)$$

In the above equation,

[M] Inertia matrix of the rotor-shaft bearing system;
[D] Matrix that takes into account of the gyroscopic effect, direct damping effect of The internal damping of the shaft material bearing damping;
[K] The shaft stiffness, bearing stiffness and circulatory effect of the internal material damping of the shaft.
{q} Nodal displacement vector for the entire system.
{f} Global force vector due to mass-unbalance.
{f_{EMA}} Force due to electromagnetic actuator.

4.4 The Proportional-Derivative Control Strategy

The proportional-derivative control action for each magnet by feeding back the rotor displacement and its derivative with gains k_p (V/m) and k_v (V s/m) respectively using co-located displacement sensors [36].
Expression of the control currents are given by

$$I_{cY} = -k_g\left(k_P v + k_v \dot{v}\right) \quad (4.8)$$

$$I_{cZ} = -k_g\left(k_P w + k_v \dot{w}\right) \quad (4.9)$$

Where,
k_g Is the power amplifier gain in (A/V). Putting these values in equations of currents in equation (4.8) & (4.9). We get

$$F_Y = -\left(k_g k_i k_P - k_S\right)v - k_g k_i k_v \dot{v} \quad (4.10)$$

$$F_Z = -\left(k_g k_i k_P - k_S\right)w - k_g k_i k_v \dot{w} \quad (4.11)$$

So magnetic exciter may be modelled to have a combined stiffness of $\left(k_g k_i k_P - k_S\right)$ and a combined damping coefficient of $k_g k_i k_v$.

4.5 Linear Quadratic Regulator (LQR)

The transfer function is transformed to a state space vector dynamic equation for state feedback control system design. To minimize the displacement of the rotor shaft system, the Linear Quadratic Regulator (LQR) based on independent mode space control techniques is designed. The control voltage for the actuators is determined by the optimal control solution of the Linear Quadratic Regulator (LQR), which is an effective and widely used linear control technique. Provided the full state vector is observable, this method can be employed to meet specific design and performance criteria. A quadratic cost function is used to minimize the performance index.

State-space model can be written as-

$$\dot{X} = A^* X + B^* U(t) \tag{4.12}$$

$$Y = CX \tag{4.13}$$

LQR optimal control theory has been used to determine the control gains. In this, the feedback control system has been designed to minimize a cost function or a performance index, which is proportional to the required measure of the system's response. The cost function used in the present case is given by:

$$J = \frac{1}{2}\int_{t_0}^{t_f} \left(\{X\}^T [Q]\{X\} + \{U\}^T [R]\{U\}\right) dt \tag{4.14}$$

Where [Q] and[R] are the semi-positive-definite and positive-definite weighting matrices on the outputs and control inputs, respectively.

The steady-state matrix Ricatti equation can be written as:

$$[A]^T [P] + [P][A] - [P][B][R]^{-1}[B][P] + [Q] = 0 \tag{4.15}$$

After solving the recatti equation using potters method, optimal gain can be written as

$$K_{lqr} = K_{opt} = [R]^{-1}[B]^T [P] \tag{4.16}$$

The Matlab command in Equation (19) is used to compute the LQR gain matrix.

$$[k, S, E] = lqr(A, B, Q, R) \tag{4.17}$$

Considering output feedback, actuation current can be written as:

$$\begin{bmatrix} I_{CY} \\ I_{CZ} \end{bmatrix} = [-K]_{lqr} * \begin{bmatrix} v \\ w \\ \dot{v} \\ \dot{w} \end{bmatrix} \tag{4.18}$$

CHAPTER 5

RESULTS AND DISCUSSIONS

Based on the above formulation, a complete MATLAB code has been developed and validated with the available results in the literatures and Different analysis has been carried out and presented in the following sub sections.

5.1 Summery of various Analyses

A composite shaft is supported on two bearings and a disk is rigidly mounted on the centre of the shaft. The supporting bearings are modelled as springs and viscous dampers. Vibration control of this rotor-shaft-bearing system due to unbalance forces has been studied using one and two electromagnetic actuators with PD control strategy. The shaft is discretized by 20 numbers of elements (it has been decided after convergence study). The total number of nodes in this model is 41. The stiffness and damping coefficients of each bearing at the both ends is considered as: K_{XX} = 1.75 x10^7 N/m, K_{XY}=0 N/m, K_{YY} = 1.75 x10^7 N/m and C_{XX} =500 Ns/m, C_{XY}=500 Ns/m, C_{XY} =500 Ns/m respectively.

5.2 Code Validation

In order to verify the FE developed code the following dimensions and mechanical properties were considered for steel shaft [36] (details of which are given in Table 5.1). In order to convergence study of the result, it has been observed that result from the present code has been achieved an excellent agreement with the already published results [36] and thus validates the correctness of the developed code. It is shown in Fig. 5.1.

Table 5.1 Mechanical Properties and Geometric dimension of Steel Rotor-shaft system [36**]**

Parameter	Shaft	Disk
Rotor shaft length (m)	1.3	
Rotor shaft diameter (mm)	100	
Young's Modulus (Gpa)	200	
Eccentricity (m)0.0002		
Density (Kg/m^3)	7800	7800
Outer diameter (m)	0.24	
Thickness (mm)	5.0	
Position from left end of rotor (m)	0.2	

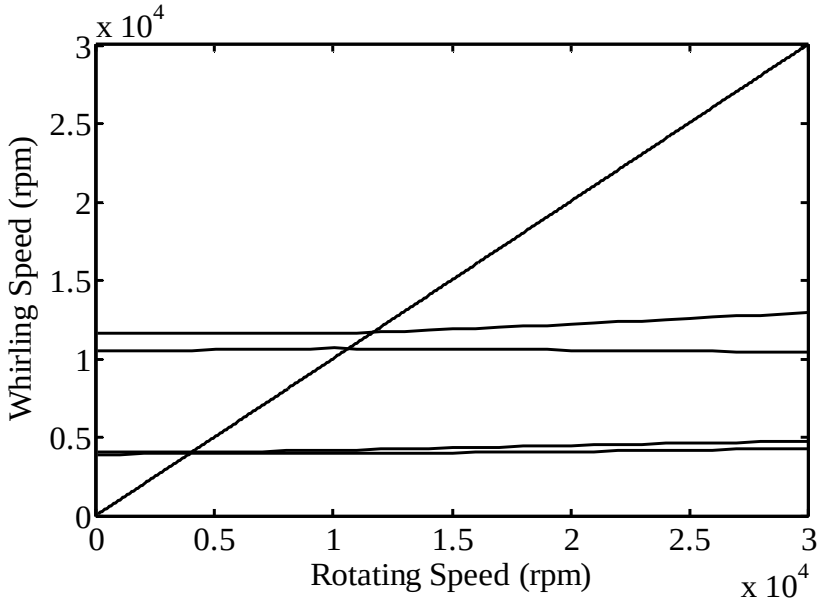

Fig.5.1: Campbell diagram of steel shaft for first two pairs of modes

5.3 Uncontrolled and controlled responses of the various composite shafts

For validation of code different types of the stacking laminated structure has been considered. Mechanical and geometrical dimension of all laminated composites are listed [20], details of which are given in Table 5.2. Rotor shaft is assumed that rotating at 15000 RPM. A disk is placed at midpoint of the shaft i.e. at the node position no. 21. First of all one actuator is placed at the node position no. 20 and response history is observed at the disk position. After then two actuators is placed at the node position nos. 20 and 22 and response history is observed at the disk position.

Table 5.2 Mechanical Properties and Geometric dimension of Composite shaft [20]

Parameter	Shaft	Disk
Rotor shaft length, L (m)	0.72	
shaft inner diameter, d_i (m)	0.028	
shaft inner diameter, d_o (m)	0.048	
Mean dia of shaft, D (m)	0.1269	
Longitudinal Young's Modulus (Gpa)	$139x10^9$	
Transverse Young's Modulus (Gpa)	$11x10^9$	
Density (Kg/m^3)	1578	
Thickness of each composite layer (m)	0.001	
Poisson's ratio	0.313	
Longitudinal shear modulus, (Gpa)	$6.05x10^9$	
Transverse shear modulus, (Gpa)	$3.78x10^9$	
Eccentricity (m)		$5x10^{-5}$
Mass of disk in Kg		2.4364
Diametrical inertia of disk in kg-m2		0.1901
Polar inertia of disk in kg-m2		0.3778

After then, result for the controlled current and the controlled force have been developed and compared with one and two actuator. The parameters for electromagnetic actuator [36] are listed in the Table.5.3

Table.5.3 Parameters used for electromagnetic actuator and PD control techniques [36]

Parameters	**value**
N	1000
$A_p(\text{cm}^2)$	5
K_p (V/m)	5000
K_v (V.s/m)	4000
α (in degree)	22.5
K_g (A/V)	2
g_o (mm)	2.5

In the following sub section result has been presented for the different stacking laminate.

5.3.1 Symmetric angle ply laminated shaft

Stacking sequence for symmetrical angle ply is considered as $[45/-45/90/-90]_{2S}$. Campbell diagram for the symmetrical angle ply rotor shaft system is shown in Fig. 5.2 and it is found that first critical speed is 3500 r.p.m. The uncontrolled displacement history for the symmetrical angle ply laminated shaft in the *v*-direction and in *w*-direction due to unbalance forces is depicted in Fig. 5.3 and 5.4. The controlled displacement histories using one actuator in *v* and *w*-directions are shows in Figs. 5.5 and 5.6 respectively. The controlled displacement history using two actuators in *v* and *w*-directions are shows in Figs. 5.7 and 5.8 respectively. Controlled currents for the present symmetrical angle ply laminated shaft using one actuator in the direction of *Y* and *Z* shown in Fig 5.9 and 5.10 respectively. Controlled currents for the present symmetrical angle ply laminated shaft using two actuators in the direction of *Y* and *Z* shown in Fig 5.11 and 5.12 respectively. Controlled force for the present symmetrical angle ply laminated shaft using one actuator in the direction of *Y* and *Z* shown in Fig 5.13 and 5.14 respectively. Controlled force for the present symmetrical angle ply laminated shaft using two actuators in the direction of *Y* and *Z* shown in Fig 5.15 and 5.16 respectively.

It has been observed from the Fig.5.3, 5.5 and 5.7 that displacement in the direction of *V* is reduced by 98.86 % using one actuator and by 99.58 % while using two actuators. Also it has been found that from the Fig.5.4, 5.6 and 5.8 the displacement in the direction of *W* is reduced by 99.36 % when using one actuator and by 99.74 % when using two actuators.

From Fig.5.9 and 5.11 it can be noticed that controlled current requirement in the direction of *Y* for two actuators is reduced almost by 53.12 % of current requirement for one actuator. From the Fig.5.10 and 5.12 the same phenomena is noticed while considering controlled current requirement in the direction of *Z* for two actuator is reduced by 59 % of current requirement for one actuator.

From the Fig.5.13 and 5.15 it can be observed that controlled force requirement in the *Y* direction is reduced by approx 66.66 % while using two actuators with respect to one actuator. Also it can be observed that from the Fig.5.14 and 5.16 the controlled force requirement in the direction of *Z* is reduced by 59.09 % while using two actuators with respect to one actuator.

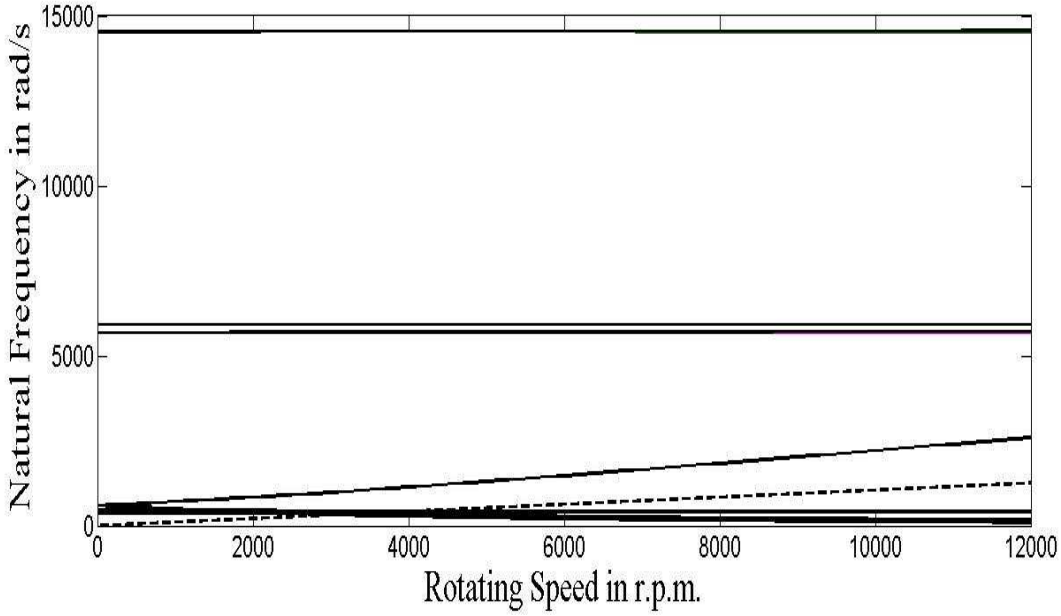

Fig. 5.2: Campbell diagram of symmetrical angle ply laminated shaft.

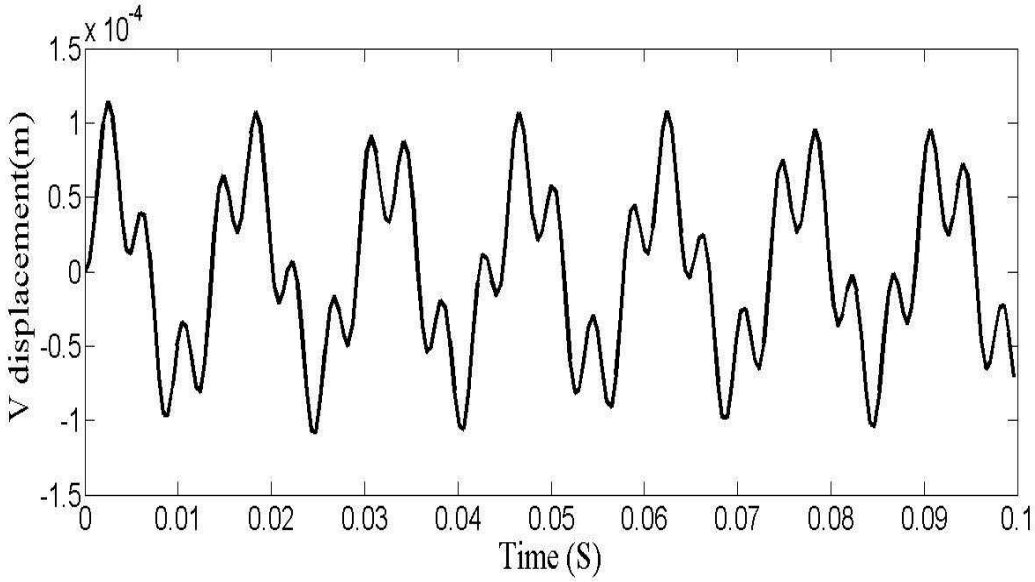

Fig. 5.3: Uncontrolled displacement history in the direction of '*V*' for the symmetrical angle ply laminated shaft.

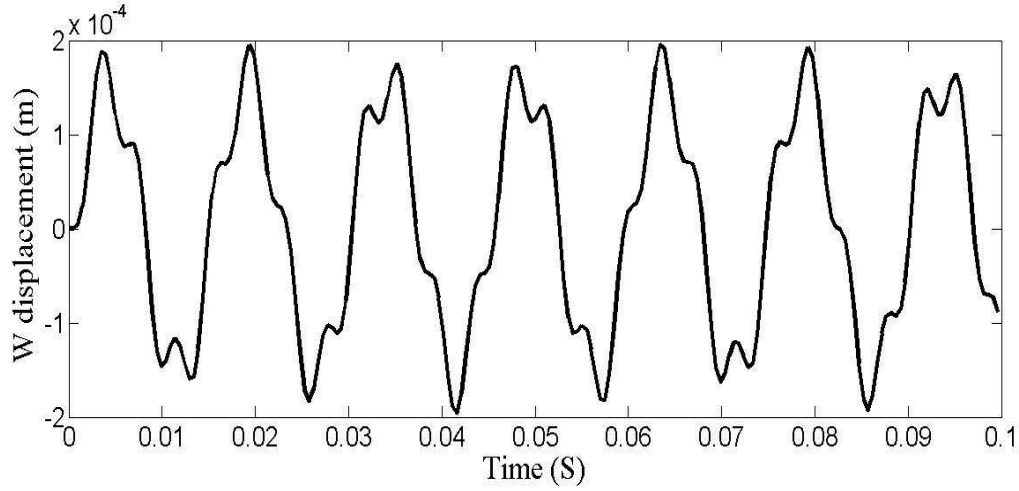

Fig. 5.4: Uncontrolled displacement history in the direction of 'w' for the symmetrical angle ply laminated shaft.

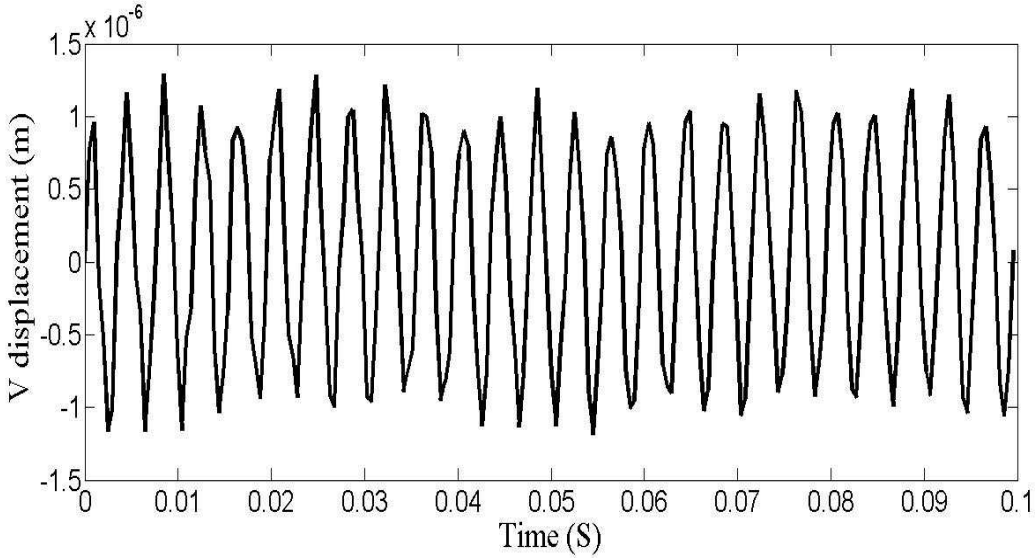

Fig.5.5: Controlled displacement history in the direction of *'V'* for the symmetrical angle ply laminated shaft using one actuator.

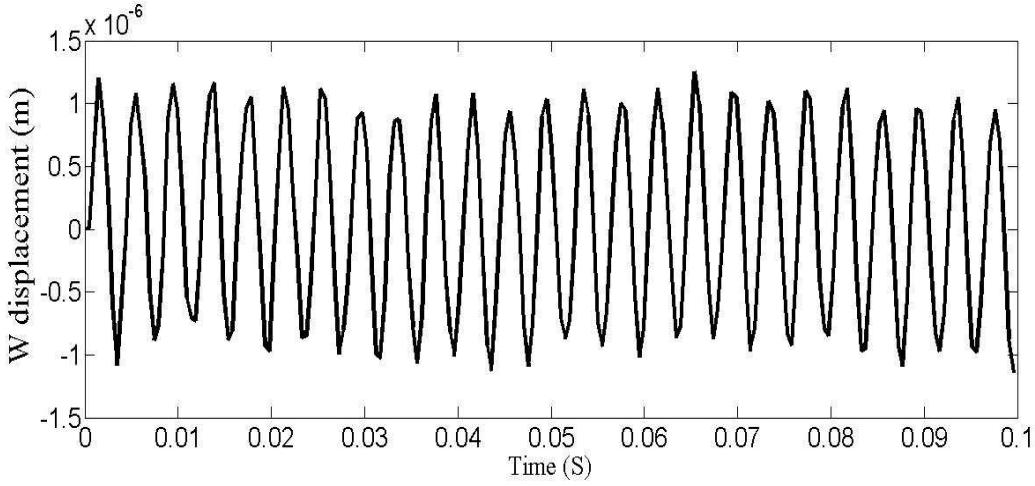

Fig.5.6: Controlled displacement history in the direction of *'W'* for the symmetrical angle ply laminated shaft using one actuator.

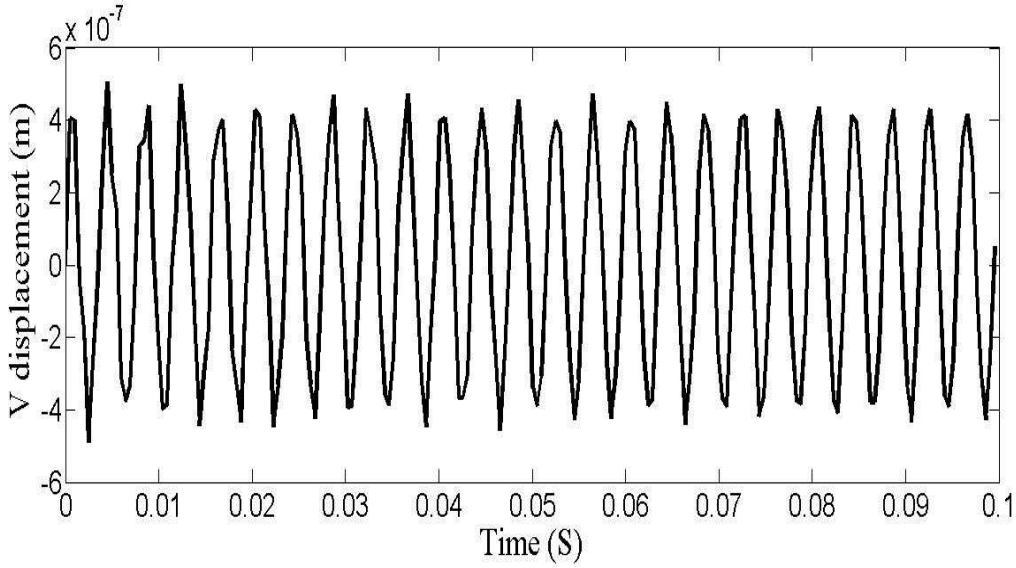

Fig.5.7: Controlled displacement history in the direction of '*V*' for the symmetrical angle ply laminated shaft using two actuators.

.

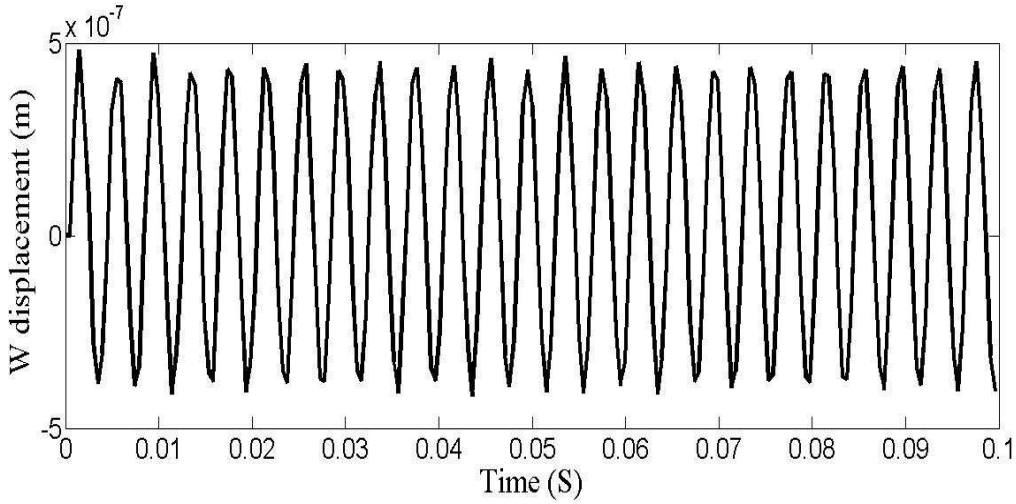

Fig.5.8: Controlled displacement history in the direction of '*W*' for the Symmetrical angle ply laminated shaft using two actuators.

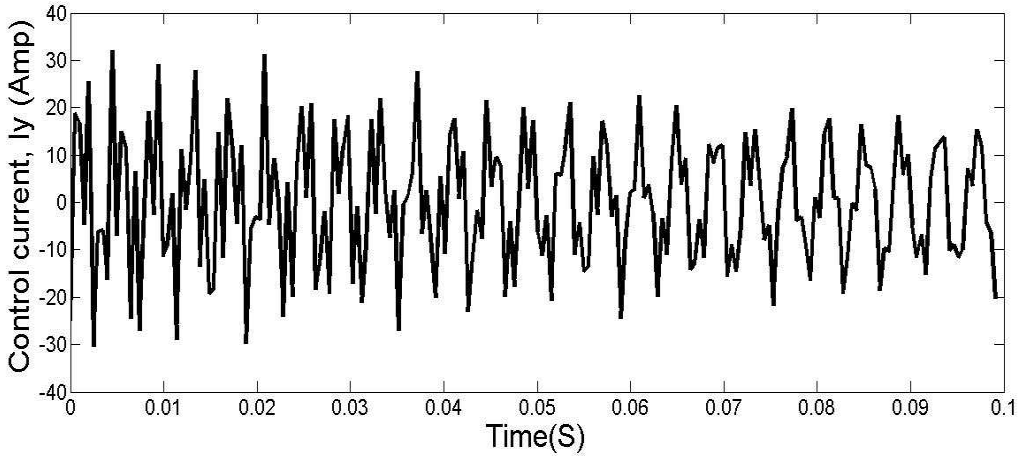

Fig.5.9: Controlled current in the direction of '*Y*' for the symmetrical angle ply laminated shaft using one actuator.

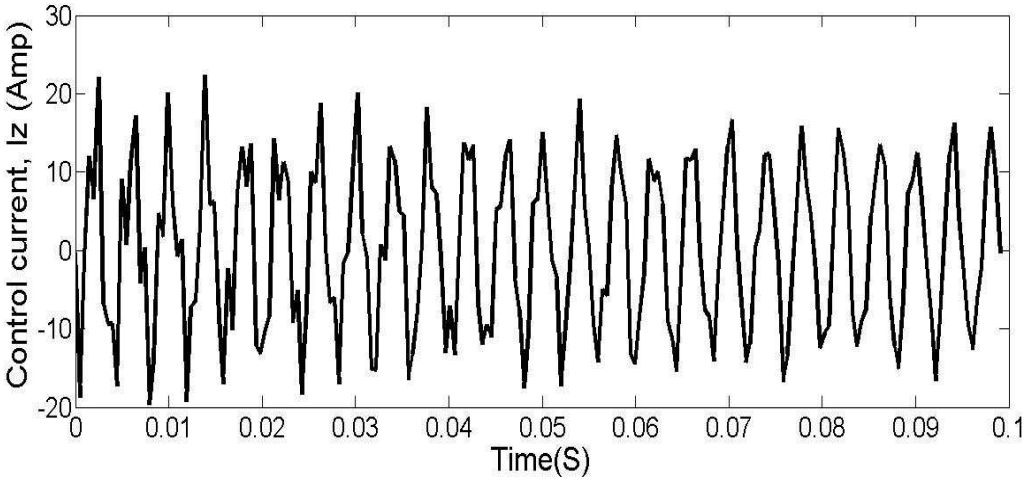

Fig.5.10: Controlled current in the direction of *'Z'* for the symmetrical angle ply laminated shaft using one actuator.

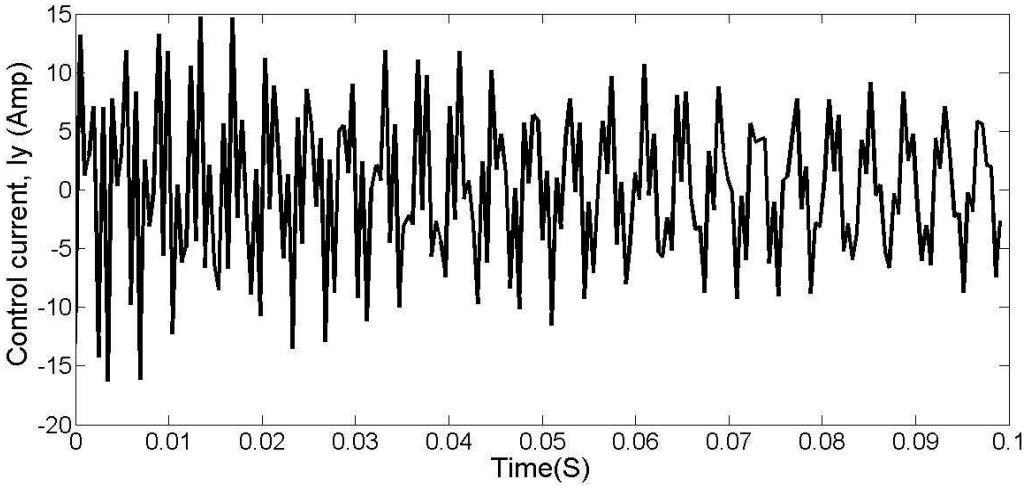

Fig.5.11: Controlled current in the direction of *'Y'* for the symmetrical angle ply laminated shaft using two actuators.

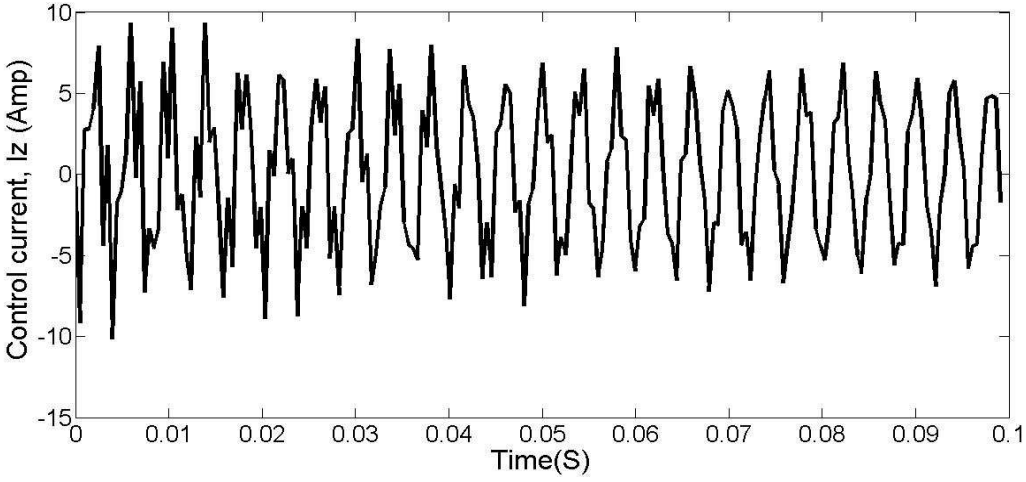

Fig.5.12: Controlled current in the direction of *'Z'* for the symmetrical angle ply laminated shaft using two actuators.

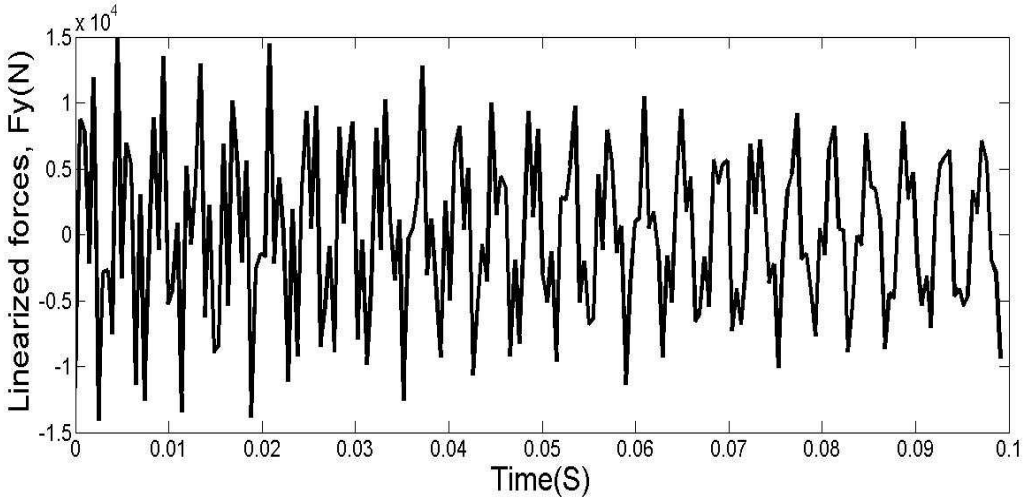

Fig.5.13: Controlled Force in the direction of '*Y*' for the symmetrical angle ply laminated shaft using one actuator.

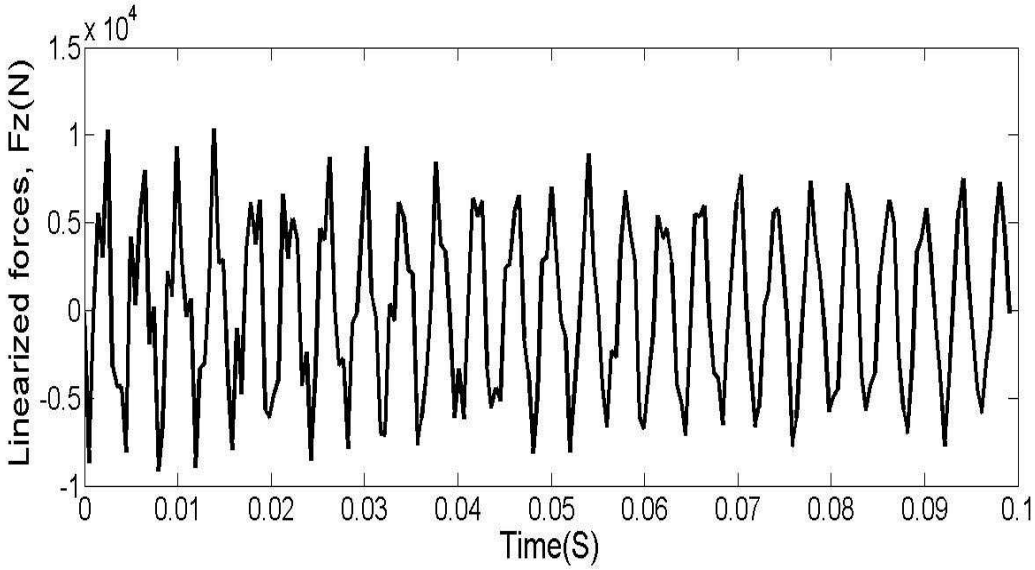

Fig.5.14: Controlled Force in the direction of '*Z*' for the symmetrical angle ply laminated shaft using one actuator.

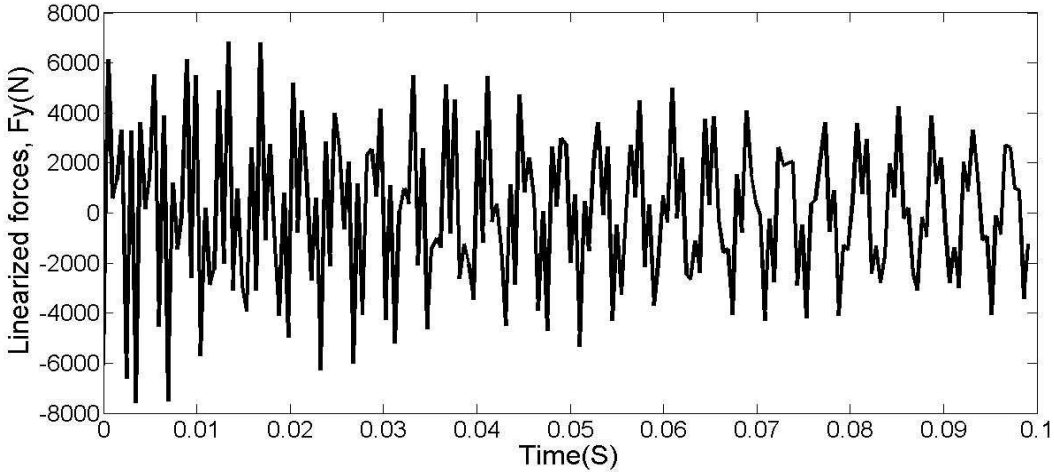

Fig.5.15: Controlled Force in the direction of '*Y*' for the symmetrical angle ply laminated shaft using two actuators.

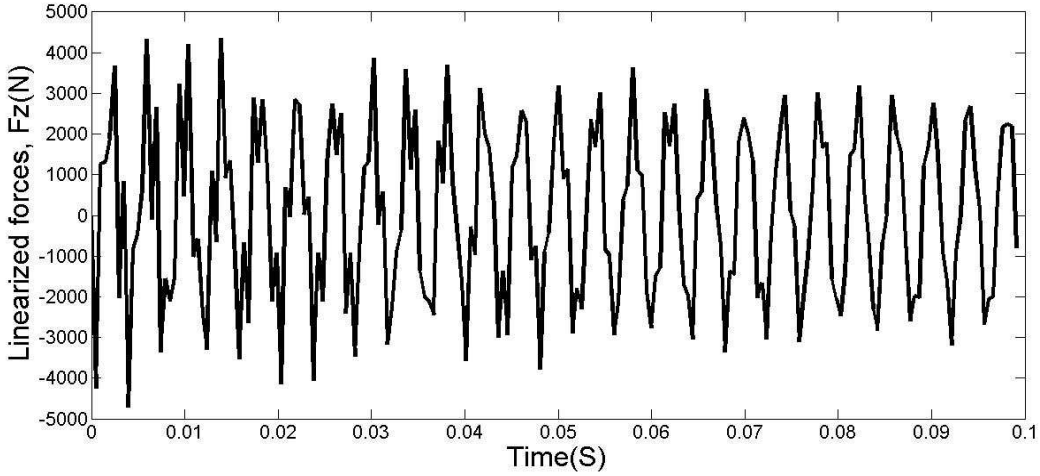

Fig.5.16: Controlled Force in the direction of '*Z*' for the symmetrical angle ply laminated shaft using two actuators.

5.3.2 Symmetric cross ply laminated shaft

Stacking sequence for symmetrical angle ply is considered as $[0/90/0/90]_{2S}$. In symmetric cross ply laminates, plies are situated at 0^o and 90°. Campbell diagram for the symmetrical angle ply rotor shaft system is shown in fig. 5.17 and it is found that first critical speed is 3000 r.p.m. The uncontrolled displacement history for the symmetrical angle ply laminated shaft in the *v*-direction and in *w*-direction due to unbalance forces is depicted in Fig. 5.18 and 5.19. The controlled displacement histories using one actuator in *v* and *w*-directions are shows in Figs. 5.20 and 5.21 respectively. The controlled displacement history using two actuators in *v* and *w*-directions are shows in Figs. 5.22 and 5.23 respectively. Controlled currents for the present symmetrical angle ply laminated shaft using one actuator in the direction of *Y* and *Z* shown in Fig 5.24 and 5.25 respectively. Controlled currents for the present symmetrical angle ply laminated shaft using two actuators in the direction of *Y* and *Z* shown in Fig 5.26 and 5.27 respectively. Controlled force for the present symmetrical angle ply laminated shaft using one actuator in the direction of *Y* and *Z* shown in Fig 5.28 and 5.29 respectively. Controlled force for the present symmetrical angle ply laminated shaft using two actuators in the direction of *Y* and *Z* shown in Fig 5.30 and 5.31 respectively.

It can be found from the Fig5.18, 5.20 and 5.22 the displacement in the direction of *V* is reduced by 97.5 % using one actuator and by 98.8 % while using two actuators. Also it has been found that from the Fig.5.19, 5.21 and 5.23 the displacement in the direction of *W* is reduced by 98.53 % when using one actuator and by 99.33 % when using two actuators.

From Fig.5.24 and 5.26 it is cleared that controlled current requirement in the direction of *Y* reduced by 41.66 % while using two actuators with respect to one actuator. From the Fig.5.25 and 5.27 also it can be observed that the controlled current requirement in the direction of *Z* is reduced by 48.78 % while using two actuators with respect to one actuator.

For the analysis of control force it can be observed from the Fig.5.28 and 5.30 the controlled force requirement in the *Y* direction is reduced by approx 46.15 % while using two actuators with respect to one actuator. Also it can be observed that from the Fig.5.29 and 5.31

the controlled force requirement in the direction of *Z* is reduced by 40.90 % while using two actuators with respect to one actuator.

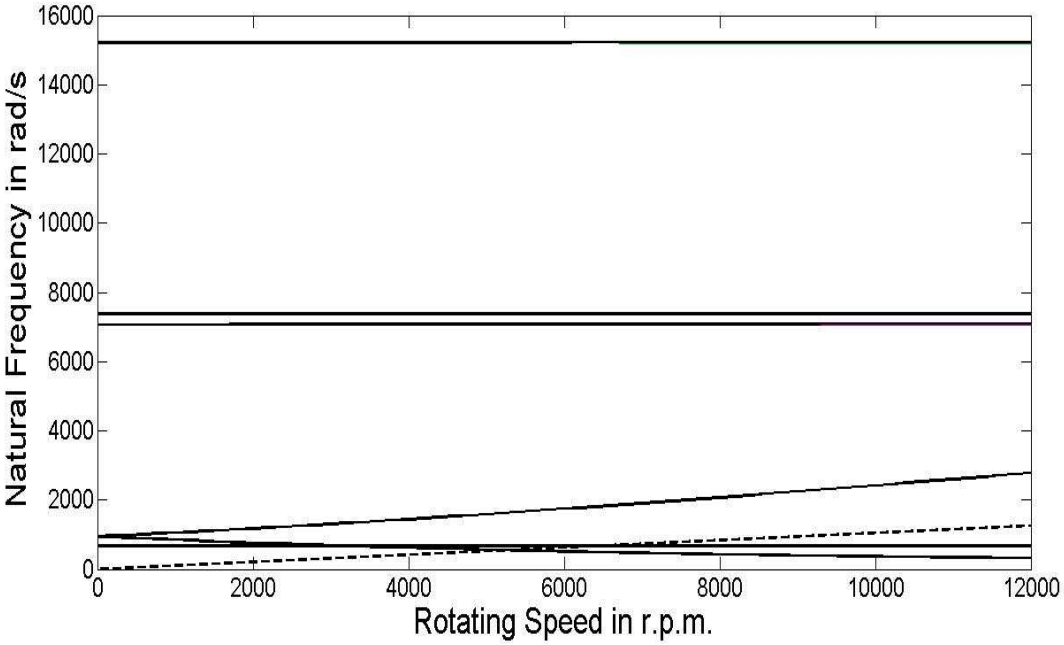

Fig. 5.17: Campbell diagram of symmetrical cross ply laminated shaft.

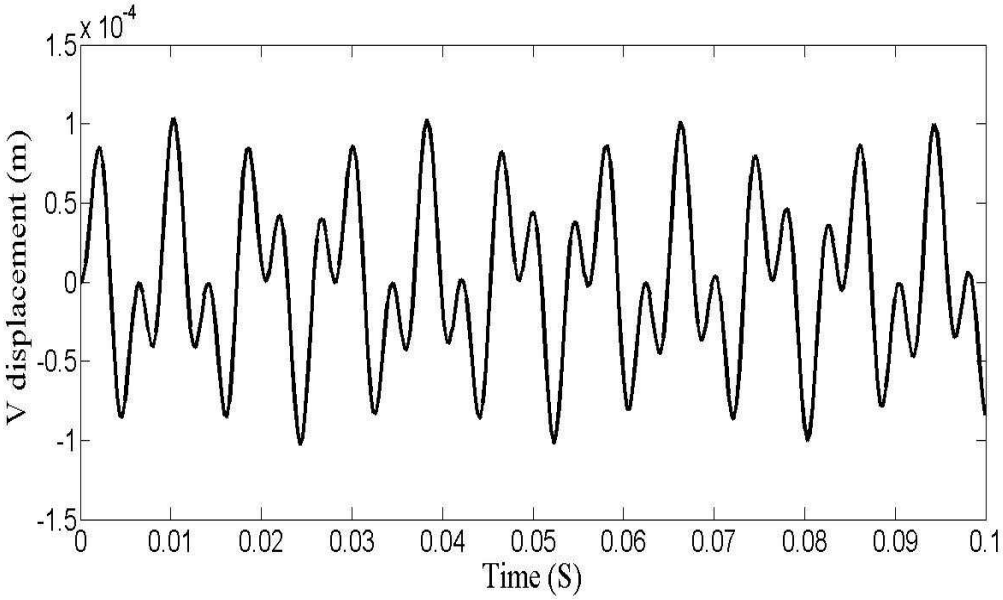

Fig. 5.18: Uncontrolled displacement history in the direction of '*V*' for the symmetrical cross ply laminated shaft.

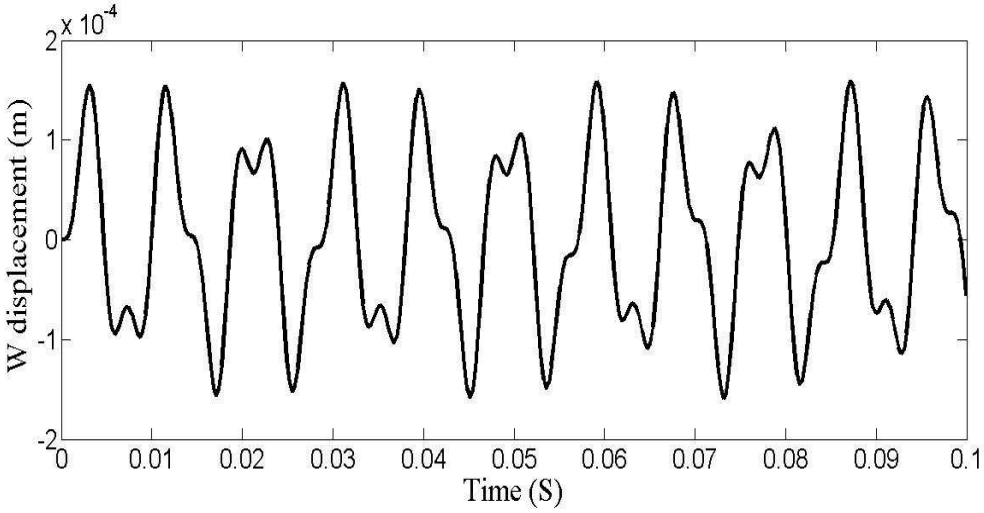

Fig. 5.19: Uncontrolled displacement history in the direction of '*W*' for the symmetrical cross ply laminated shaft.

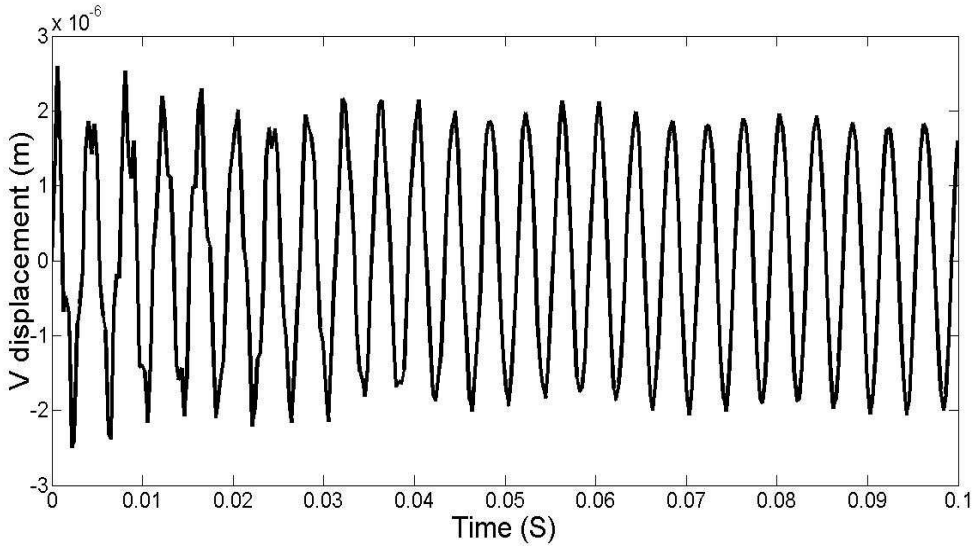

Fig. 5.20: Controlled displacement history in the direction of '*V*' for the symmetrical cross ply laminated shaft using one actuator.

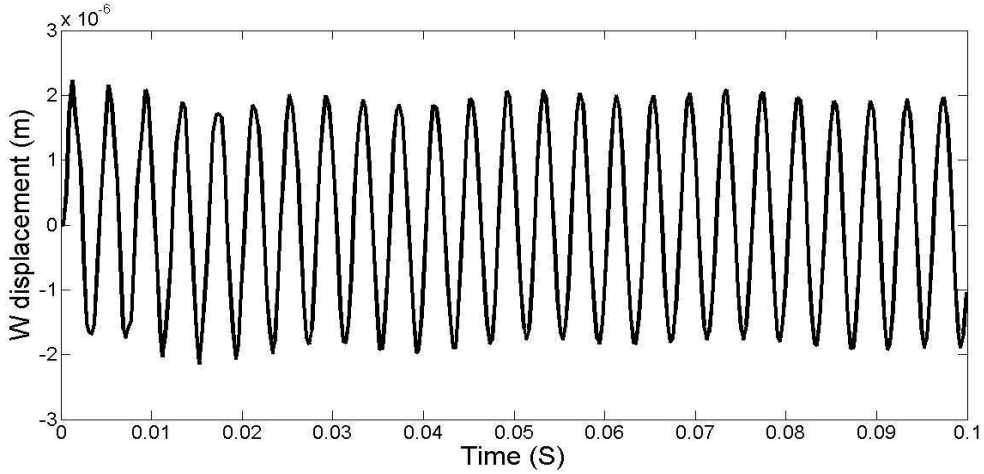

Fig. 5.21: Controlled displacement history in the direction of '*W*' for the symmetrical cross ply laminated shaft using one actuator.

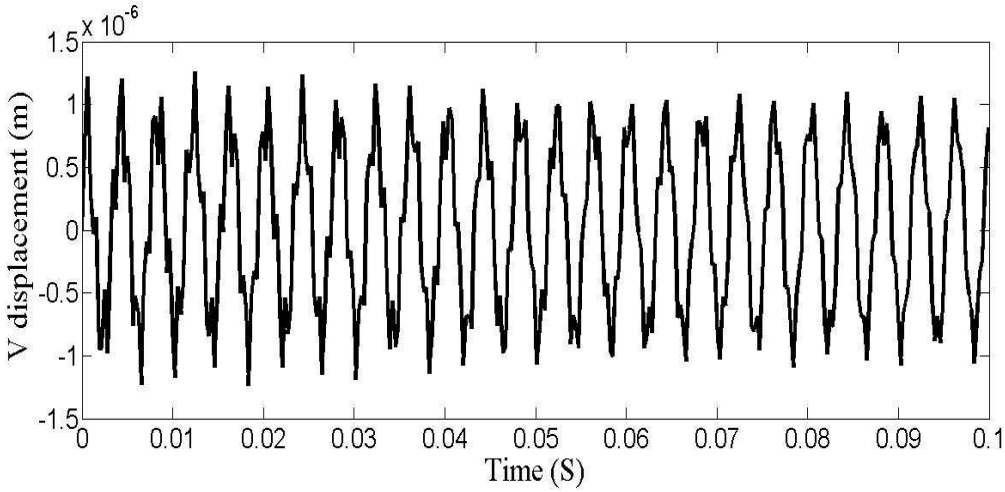

Fig. 5.22: Controlled displacement history in the direction of '*V*' for the symmetrical cross ply laminated shaft using two actuators.

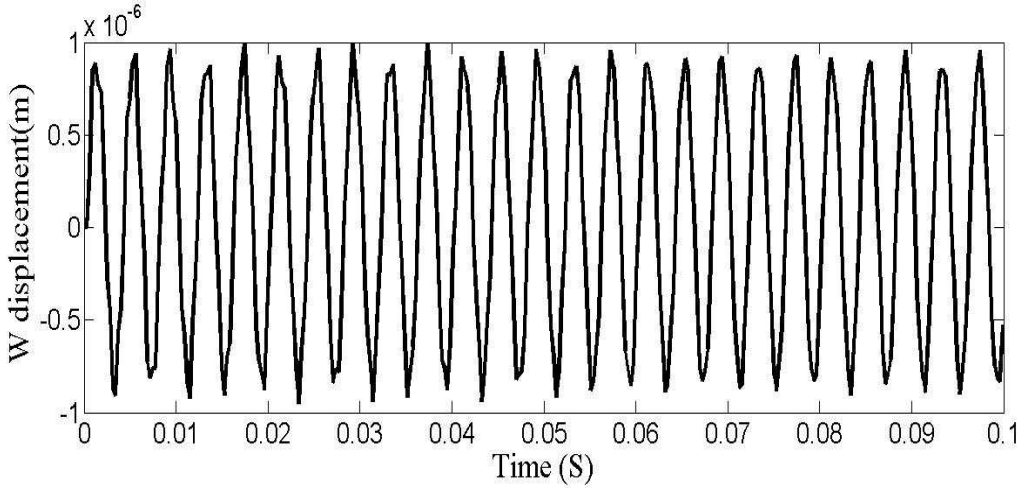

Fig. 5.23: Controlled displacement history in the direction of '*W*' for the symmetrical cross ply laminated shaft using two actuators.

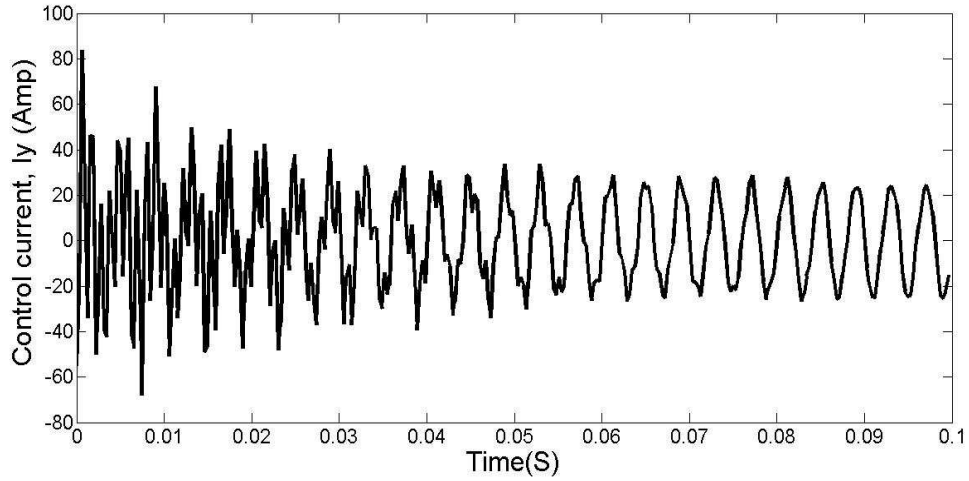

Fig.5.24: Controlled current in the direction of '*Y*' for the symmetrical cross ply laminated shaft using one actuator.

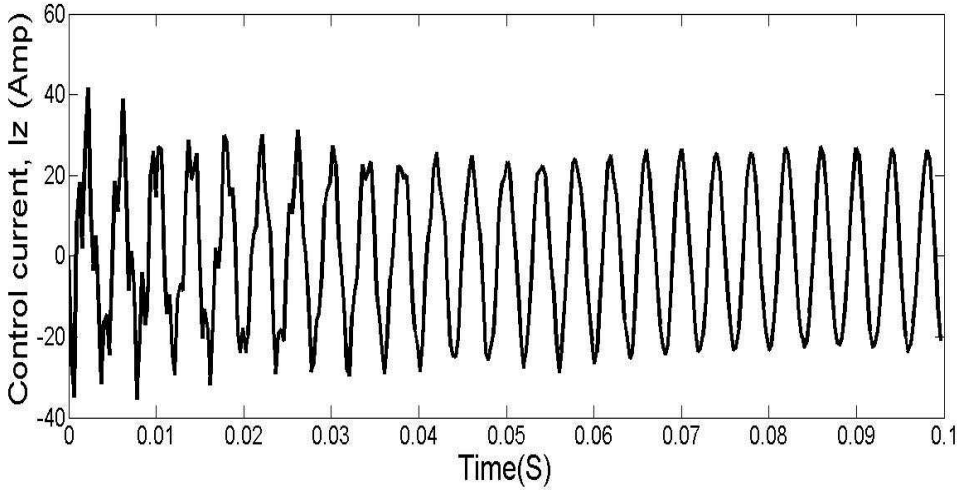

Fig.5.25: Controlled current in the direction of '*Z*' for the symmetrical cross ply laminated shaft using one actuator.

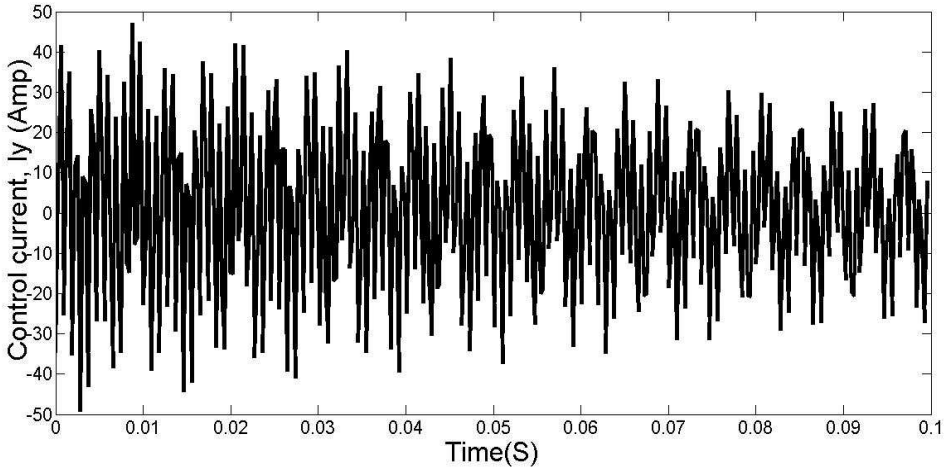

Fig.5.26: Controlled current in the direction of '*Y*' for the symmetrical cross ply laminated shaft using two actuators.

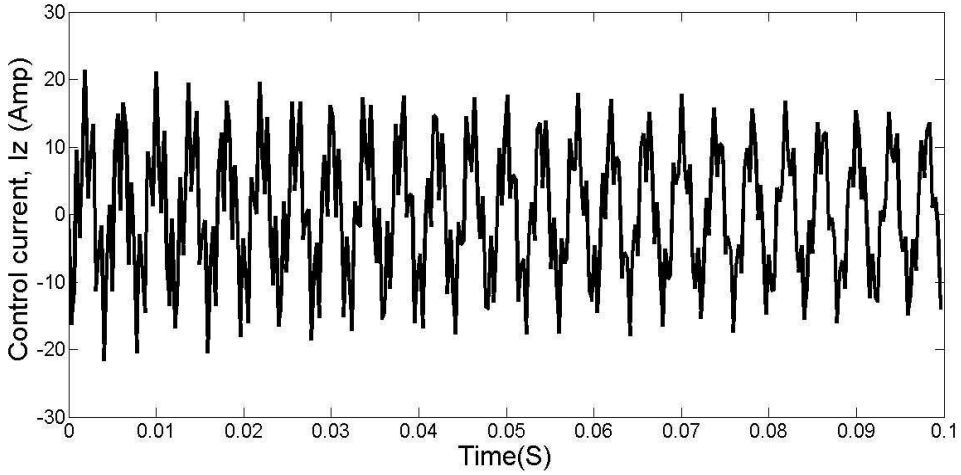

Fig.5.27: Controlled current in the direction of '*Z*' for the symmetrical cross ply laminated shaft using two actuators.

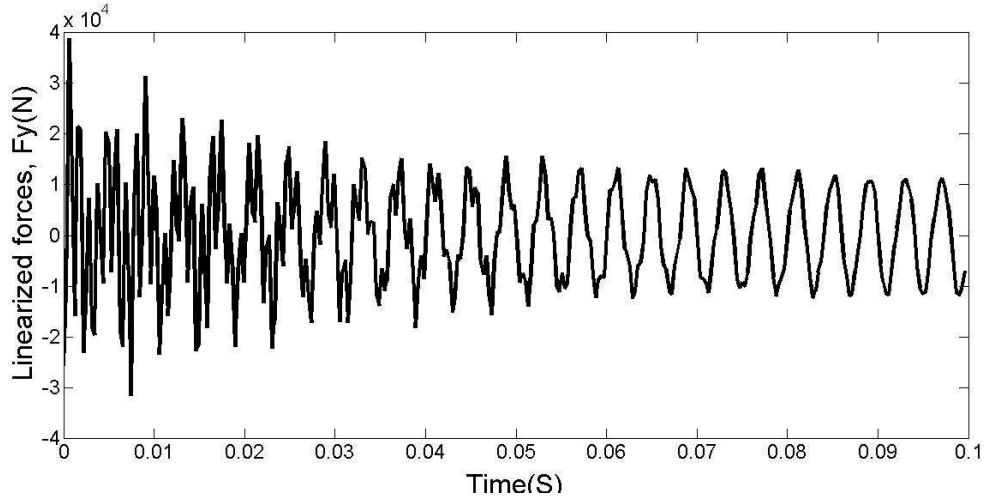

Fig.5.28: Controlled Force in the direction of *'Y'* for the symmetrical cross ply laminated shaft using one actuator.

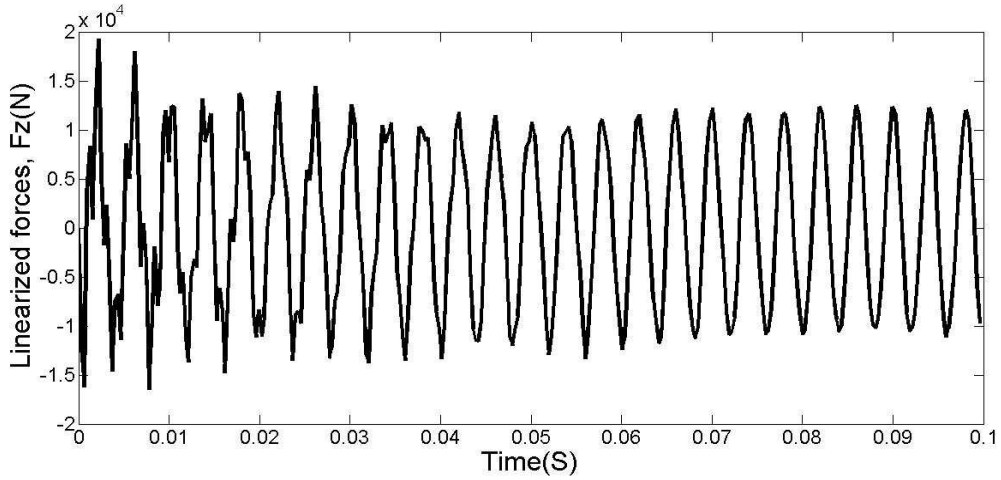

Fig.5.29: Controlled Force in the direction of *'Z'* for the symmetrical cross ply laminated shaft using one actuator.

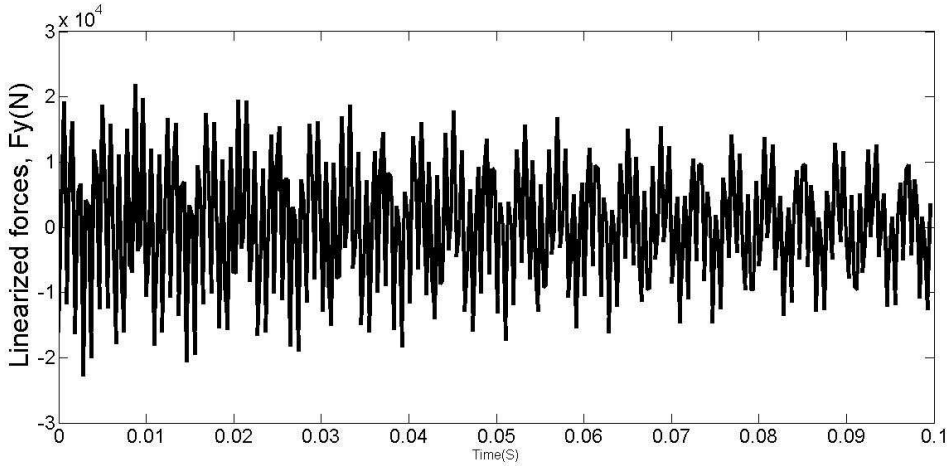

Fig.5.30: Controlled Force in the direction of *'Y'* for the symmetrical cross ply laminated shaft using two actuators.

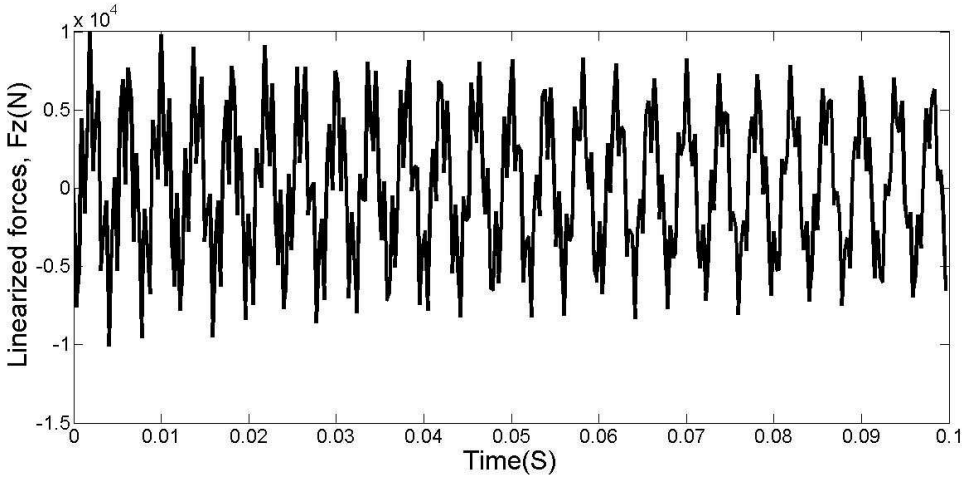

Fig.5.31: Controlled Force in the direction of *'Z'* for the symmetrical cross ply laminated shaft using two actuators.

5.3.3 Anti-symmetric cross ply laminated shaft

Stacking sequence for anti-symmetrical cross ply is considered as [0/-90/0/90/0/-90/0/90]$_{2S}$. In anti-symmetric cross ply laminates, plies are situated at 0^o and 90°. Let us consider for 0^o ply situated at a distance *z* above the reference plane, there is one ply 90^o of identical characteristics, made of the same material, same thickness below the reference plane. Campbell diagram for the symmetrical angle ply rotor shaft system is shown in fig. 5.32 and it is found that first critical speed is 300 r.p.m. The uncontrolled displacement history for the symmetrical angle ply laminated shaft in the *v*-direction and in *w*-direction due to unbalance forces is depicted in Fig. 5.33 and 5.34. The controlled displacement histories using one actuator in *v* and *w*-directions are shows in Figs. 5.35 and 5.36 respectively. The controlled displacement history using two actuators in *v* and *w*-directions are shows in Figs. 5.37 and 5.38 respectively. Controlled currents for the present symmetrical angle ply laminated shaft using one actuator in the direction of *Y* and *Z* shown in Fig 5.39 and 5.40 respectively. Controlled currents for the present symmetrical angle ply laminated shaft using two actuators in the direction of *Y* and *Z* shown in Fig 5.41 and 5.42 respectively. Controlled force for the present symmetrical angle ply laminated shaft using one actuator in the direction of *Y* and *Z* shown in Fig 5.43 and 5.44 respectively. Controlled force for the present symmetrical angle ply laminated shaft using two actuators in the direction of *Y* and *Z* shown in Fig 5.45 and 5.46 respectively.

It can be noticed from the Fig.5.33, 5.35 and 5.37 the displacement in the direction of *V* is reduced by 97.4 % using one actuator and by 98.6 % while using two actuators. Also it has been found that from the Fig.5.34, 5.36 and 5.38 the displacement in the direction of *W* is reduced by 98.40 % when using one actuator and by 99.30 % when using two actuators.

From Fig.5.39 and 5.41 it is cleared that controlled current requirement in the direction of *Y* reduced by 41.66 % while using two actuators with respect to one actuator. From the Fig.5.40 and 5.42 also it can be observed that the controlled current requirement in the direction of *Z* is reduced by 48.78 % while using two actuators with respect to one actuator.

For the analysis of control force it can be observed from the Fig.5.43 and 5.45 the controlled force requirement in the *Y* direction is reduced by approx 46.15 % while using two actuators with respect to one actuator. Also it can be observed that from the Fig.5.44 and 5.46 the controlled force requirement in the direction of *Z* is reduced by 40.90 % while using two actuators with respect to one actuator.

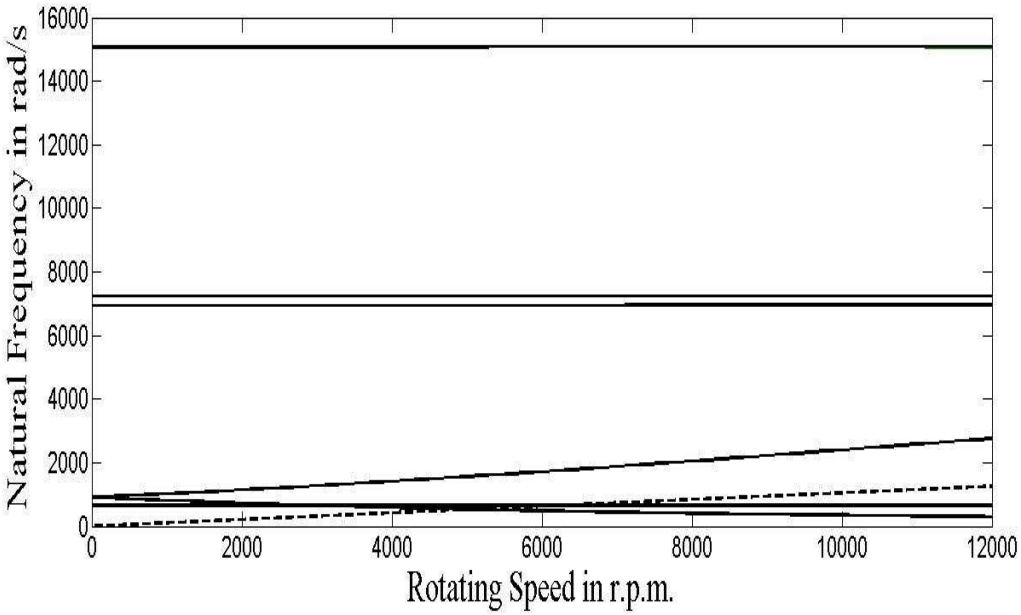

Fig. 5.32: Campbell diagram of anti-symmetrical cross ply laminated shaft.

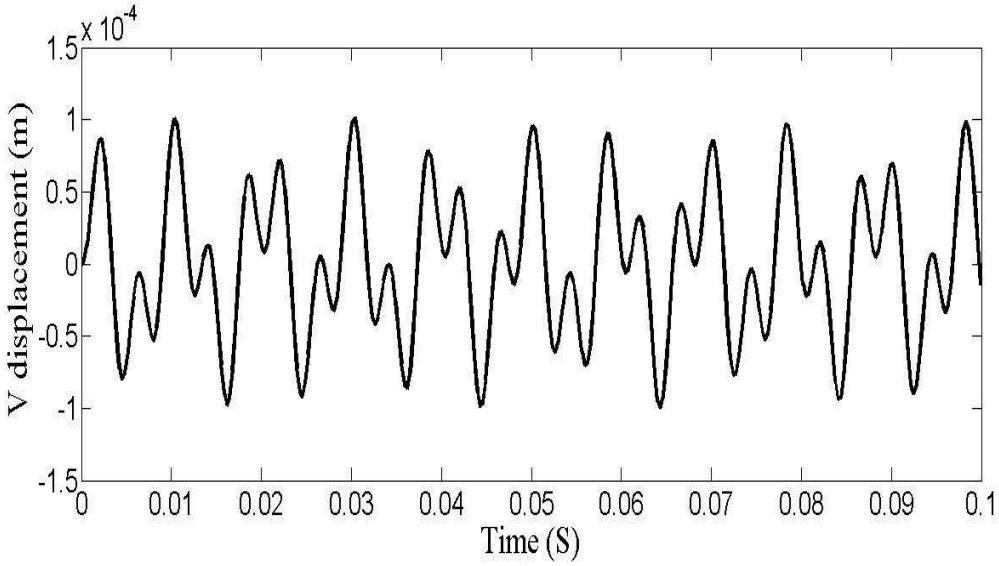

Fig. 5.33: Uncontrolled displacement history in the direction of '*V*' for the anti-symmetrical angle ply laminated shaft.

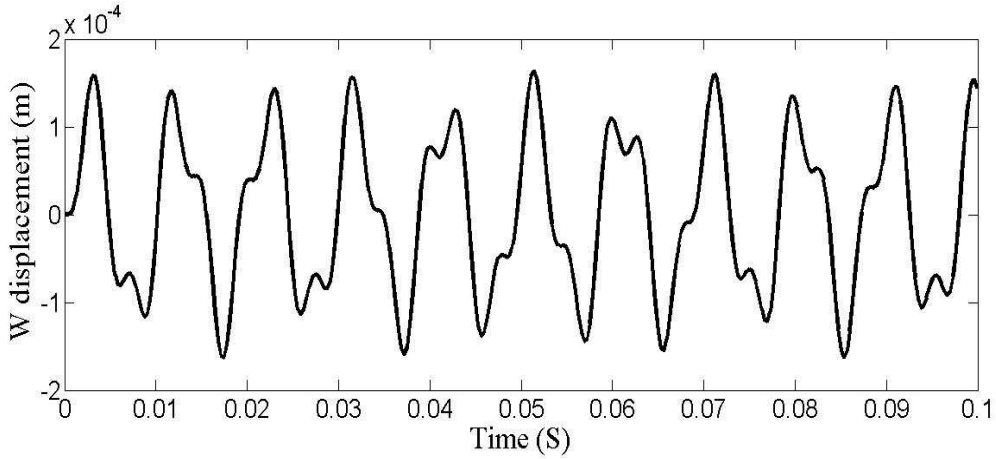

Fig. 5.34: Uncontrolled displacement history in the direction of 'W' for the anti-symmetrical angle ply laminated shaft.

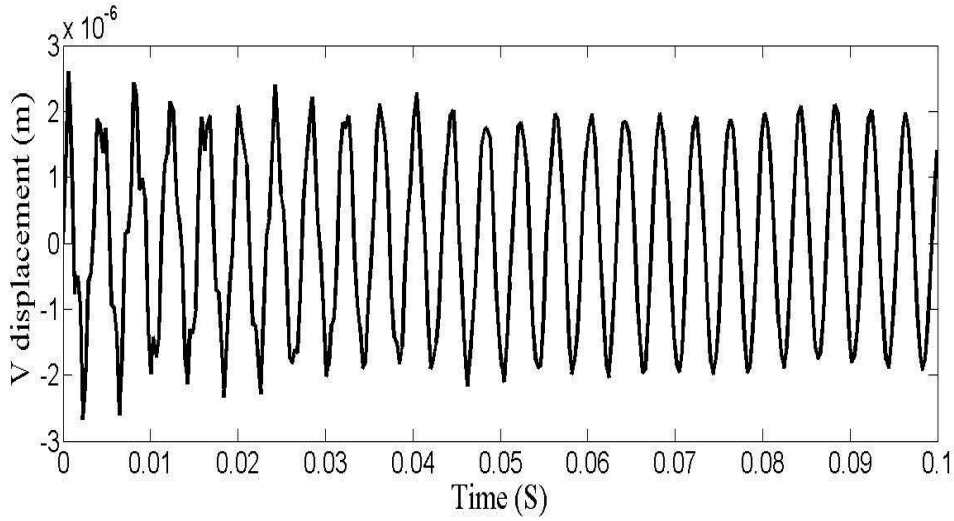

Fig. 5.35: Controlled displacement history in the direction of '*V*' for the anti-symmetrical angle ply laminated shaft using one actuator.

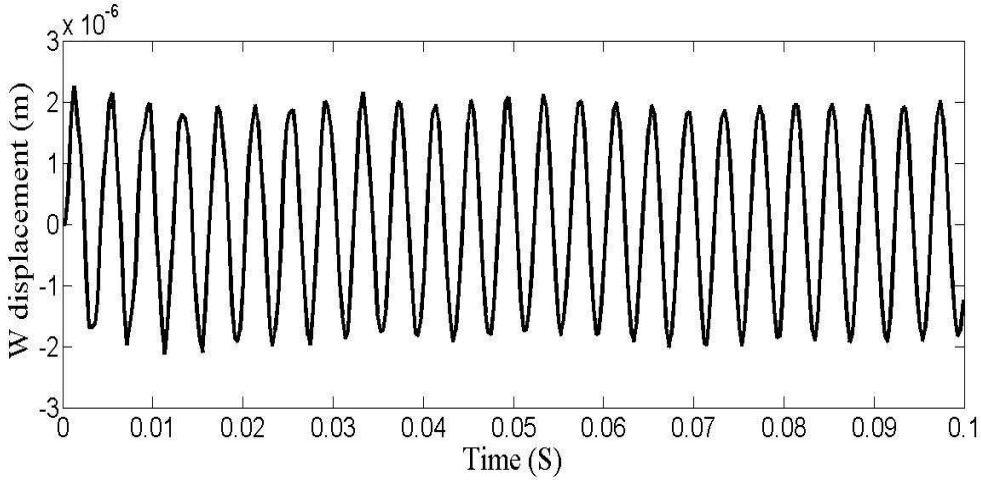

Fig. 5.36: Controlled displacement history in the direction of '*W*' for the anti-symmetrical angle ply laminated shaft using one actuator.

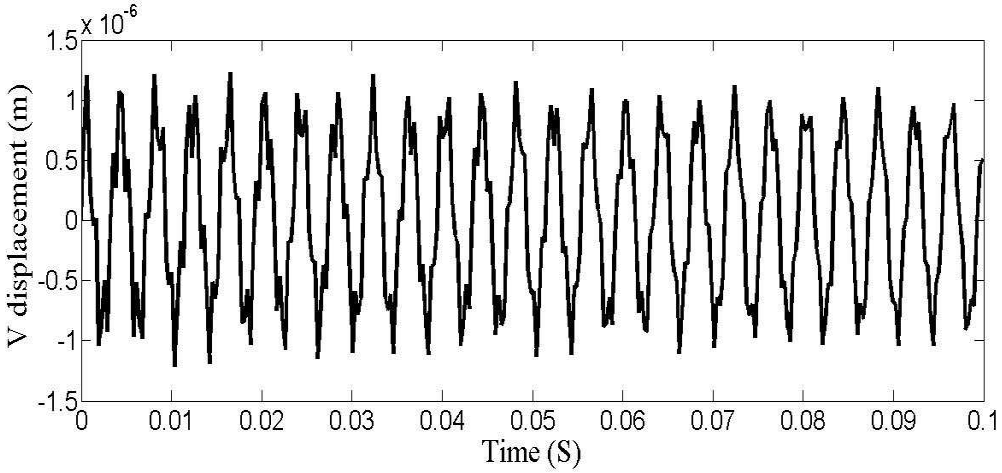

Fig. 5.37: Controlled displacement history in the direction of '*V*' for the anti-symmetrical angle ply laminated shaft using two actuators.

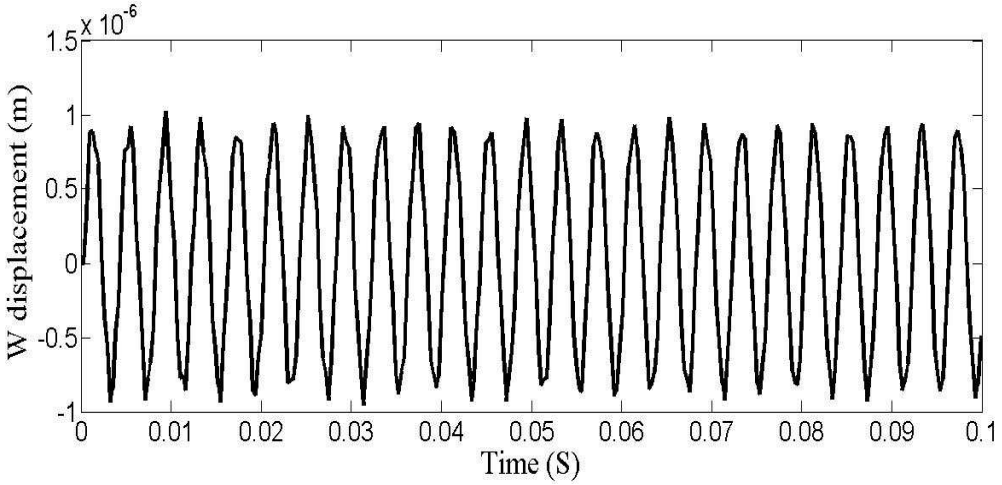

Fig. 5.38: Controlled displacement history in the direction of '*W*' for the anti-symmetrical angle ply laminated shaft using two actuators.

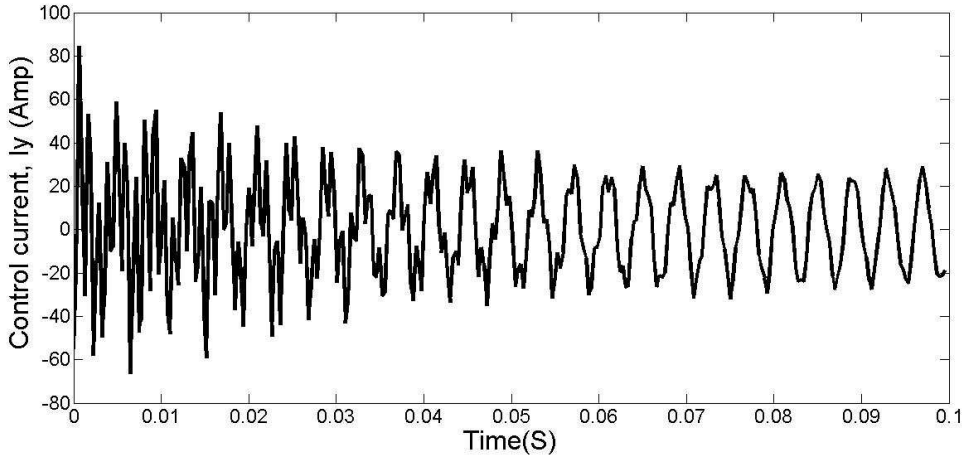

Fig.5.39: Controlled current in the direction of '*Y*' for the anti-symmetrical cross ply laminated shaft using one actuator.

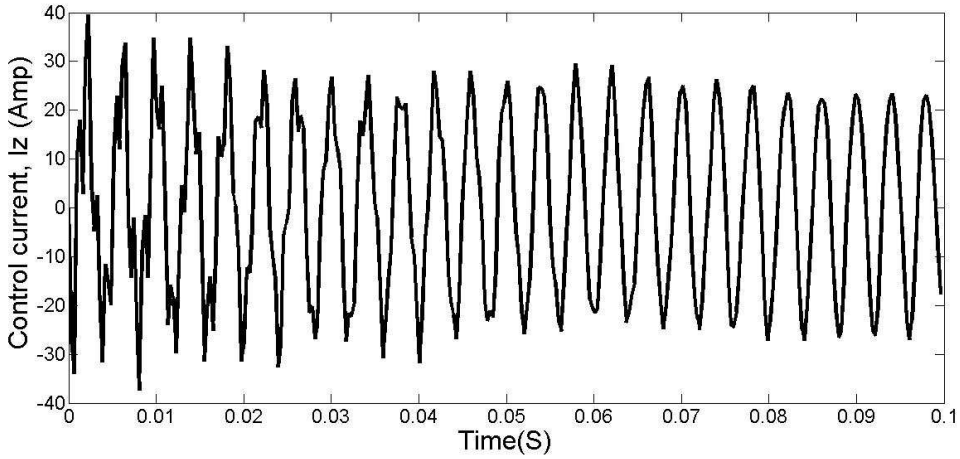

Fig.5.40: Controlled current in the direction of '*W*' for the anti-symmetrical cross ply laminated shaft using one actuator.

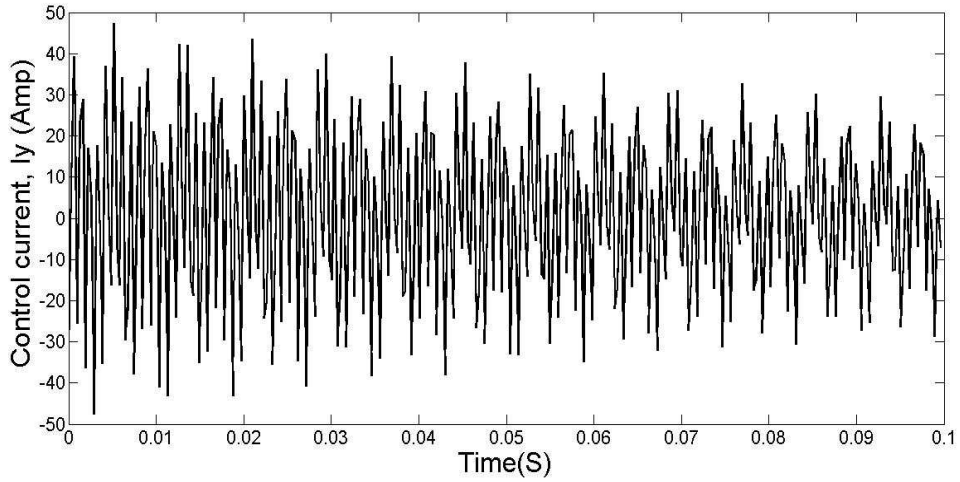

Fig.5.41: Controlled current in the direction of '*Y*' for the anti-symmetrical cross ply laminated shaft using two actuators.

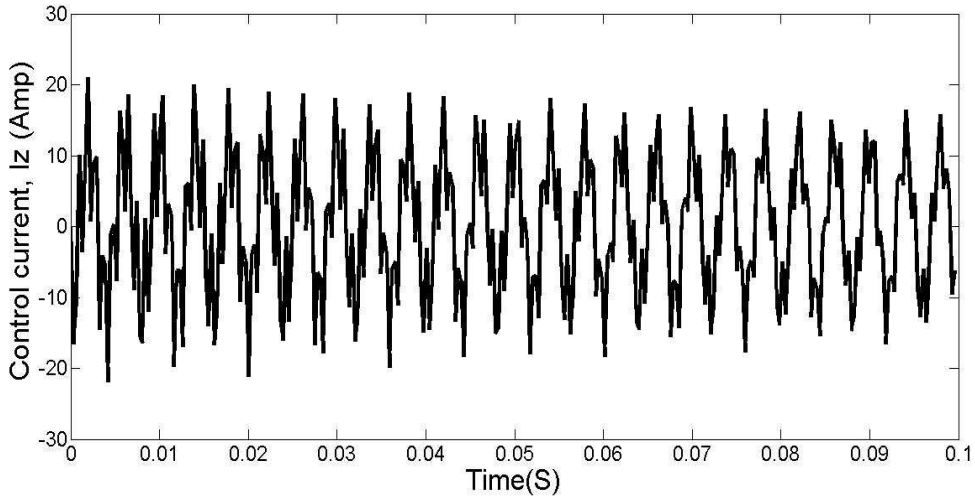

Fig.5.42: Controlled current in the direction of '*W*' for the anti-symmetrical cross ply laminated shaft using two actuators.

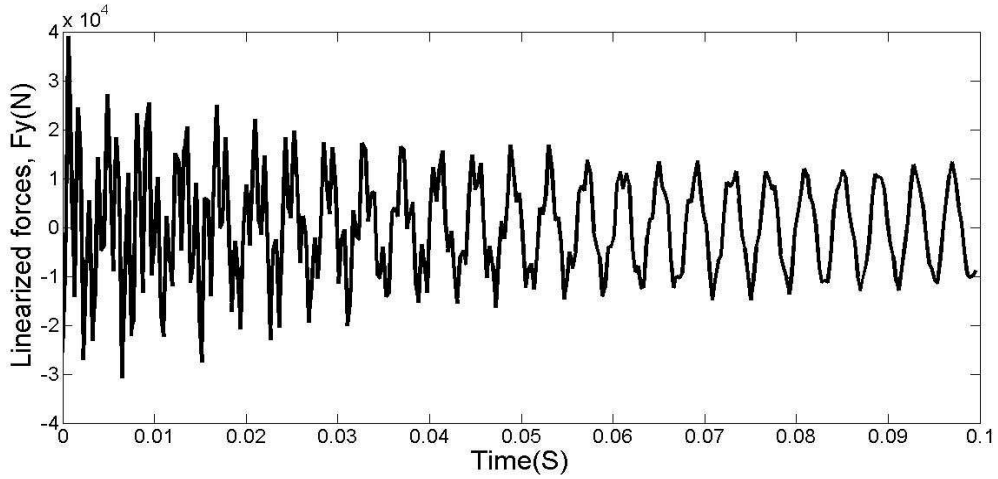

Fig.5.43: Controlled Force in the direction of *'Y'* for the anti-symmetrical cross ply laminated shaft using one actuator.

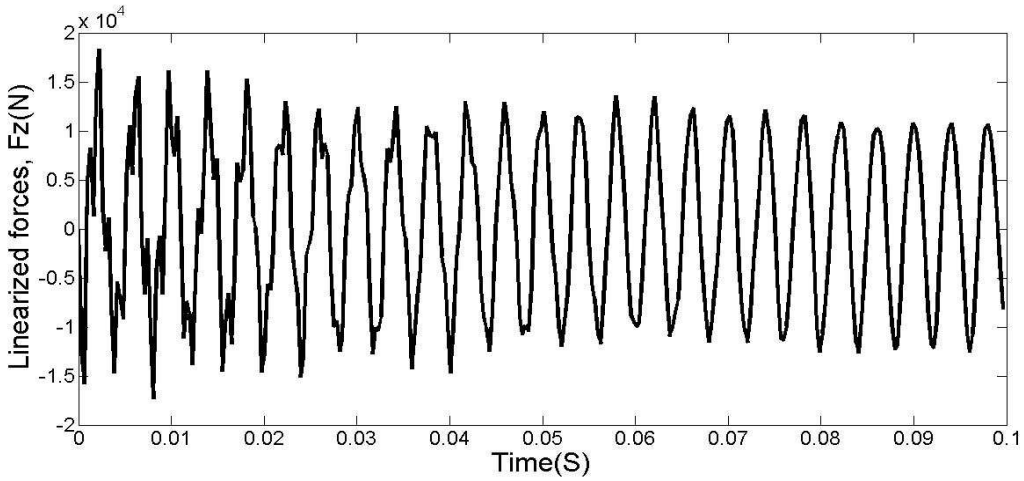

Fig.5.44: Controlled Force in the direction of *'Z'* for the anti-symmetrical cross ply laminated shaft using one actuator.

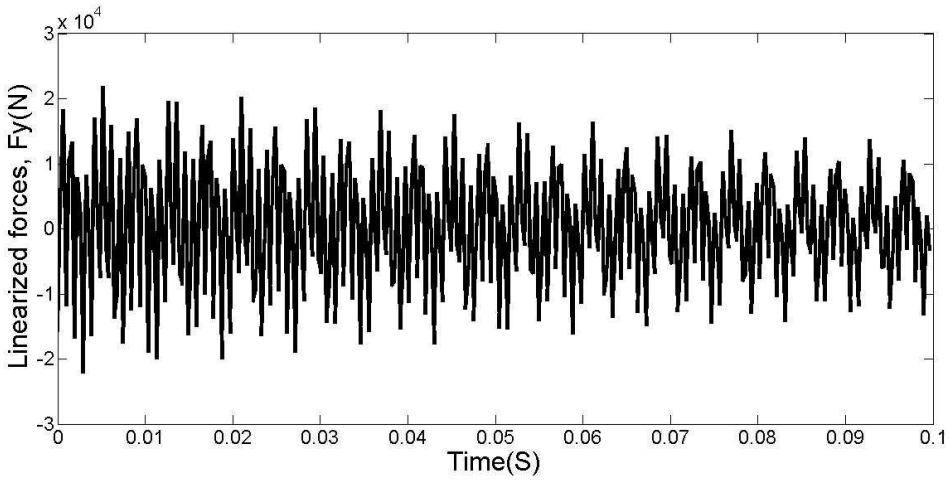

Fig.5.45: Controlled Force in the direction of *'Y'* for the anti-symmetrical cross ply laminated shaft using two actuators.

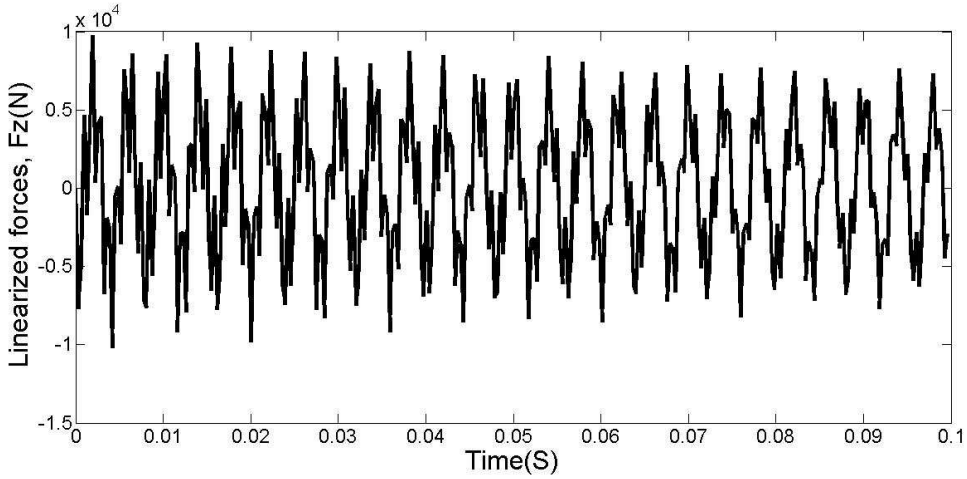

Fig.5.46: Controlled Force in the direction of *'Z'* for the anti-symmetrical cross ply laminated shaft using two actuators.

5.3.4 Quasi-isotropic laminated shaft

Stacking sequence for quasi-isotropic ply is considered as $[0/-45/45/90]_{2S}$. This is the combination of specially and generally orthotropic plies.Campbell diagram for the symmetrical angle ply rotor shaft system is shown in fig. 5.47 and it is found that first critical speed is 3200 r.p.m. The uncontrolled displacement history for the symmetrical angle ply laminated shaft in the *v*-direction and in *w*-direction due to unbalance forces is depicted in Fig. 5.48 and 5.49. The controlled displacement histories using one actuator in *v* and *w*-directions are shows in Figs. 5.50 and 5.51 respectively. The controlled displacement history using two actuators in *v* and *w*-directions are shows in Figs. 5.52 and 5.53 respectively. Controlled currents for the present symmetrical angle ply laminated shaft using one actuator in the direction of *Y* and *Z* shown in Fig 5.54 and 5.55 respectively. Controlled currents for the present symmetrical angle ply laminated shaft using two actuators in the direction of *Y* and *Z* shown in Fig 5.56 and 5.57 respectively. Controlled force for the present symmetrical angle ply laminated shaft using one actuator in the direction of *Y* and *Z* shown in Fig 5.58 and 5.59 respectively. Controlled force for the present symmetrical angle ply laminated shaft using two actuators in the direction of *Y* and *Z* shown in Fig 5.60 and 5.61respectively.

It can be noticed from the Fig.5.48, 5.50 and 5.52 the displacement in the direction of *V* is reduced by 98.9 % using one actuator and by 99.55 % while using two actuators. Also it has been found that from the Fig.5.49, 5.51 and 5.53 the displacement in the direction of *W* is reduced by 99.38 % when using one actuator and by 99.76 % when using two actuators.

From Fig.5.54 and 5.56 it is cleared that controlled current requirement in the direction of *Y* reduced by 30 % while using two actuators with respect to one actuator. From the Fig.5.55 and 5.57 also it can be observed that the controlled current requirement in the direction of *Z* is reduced by 50 % while using two actuators with respect to one actuator.

For the analysis of control force it can be observed from the Fig.5.58 and 5.60 the controlled force requirement in the *Y* direction is reduced by approx 35.7 % while using two actuators with respect to one actuator. Also it can be observed that from the Fig.5.59 and 5.61

the controlled force requirement in the direction of *Z* is reduced by 50.58 % while using two actuators with respect to one actuator.

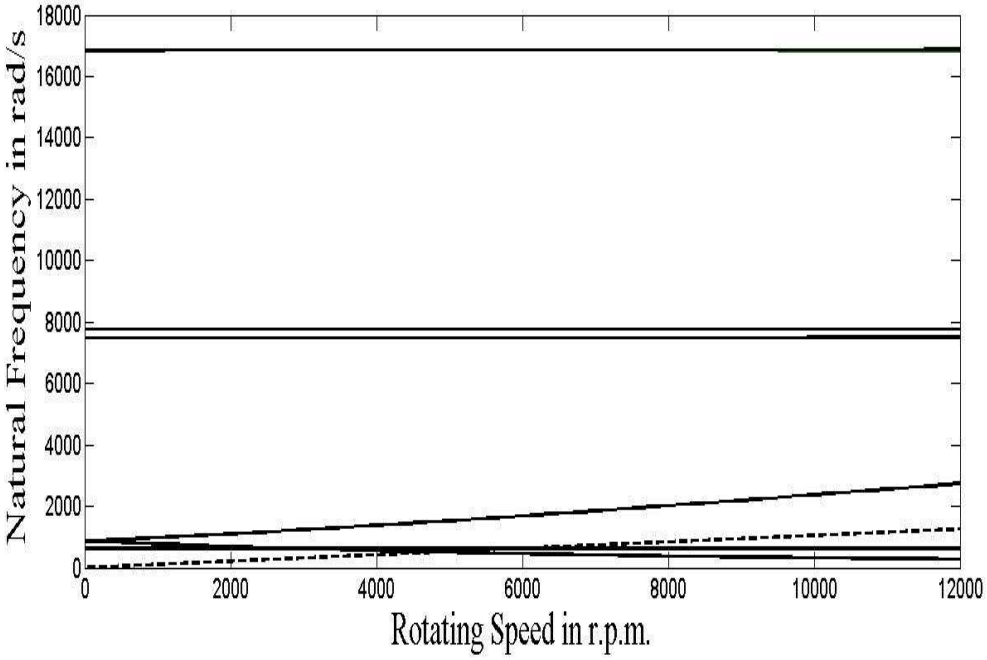

Fig. 5.47: Campbell diagram of quasi-isotropic ply laminated shaft

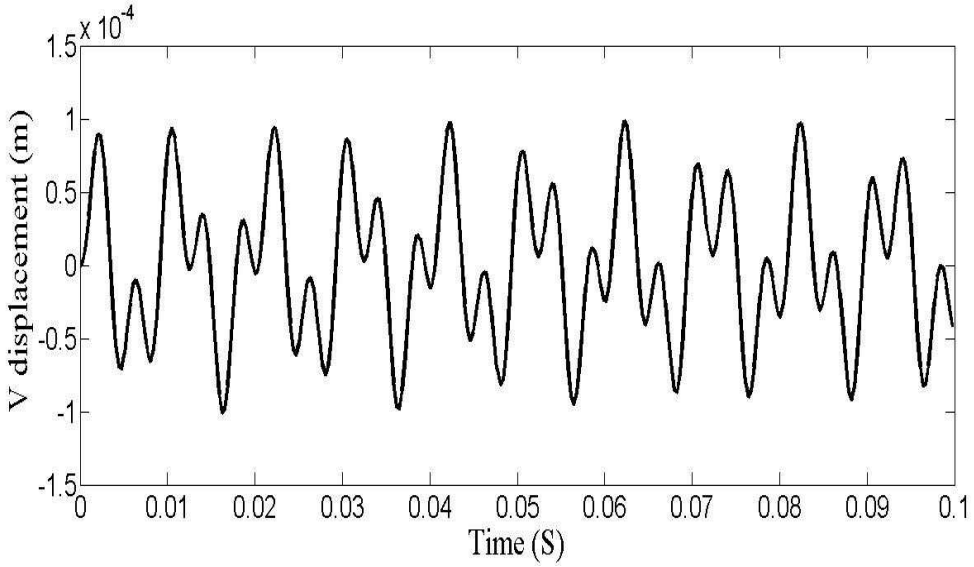

Fig. 5.48: Uncontrolled displacement history in the direction of '*V*' for the quasi-isotropic ply laminated shaft.

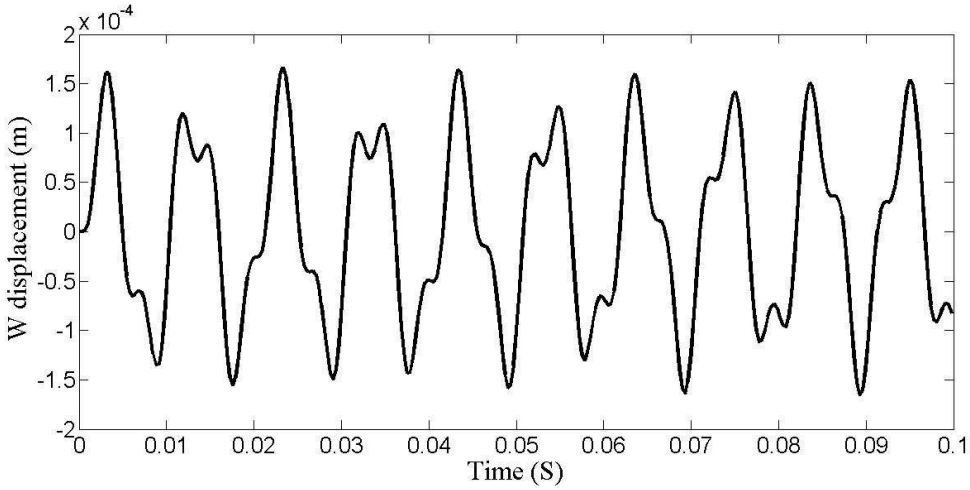

Fig. 5.49: Uncontrolled displacement history in the direction of '*W*' for the quasi-isotropic ply laminated shaft.

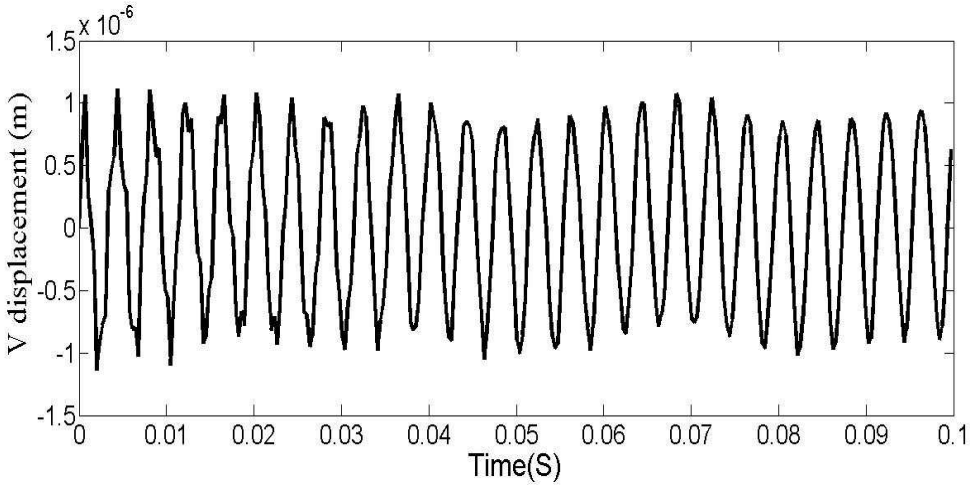

Fig. 5.50: Controlled displacement history in the direction of '*V*' for the quasi-isotropic ply laminated shaft using one actuator.

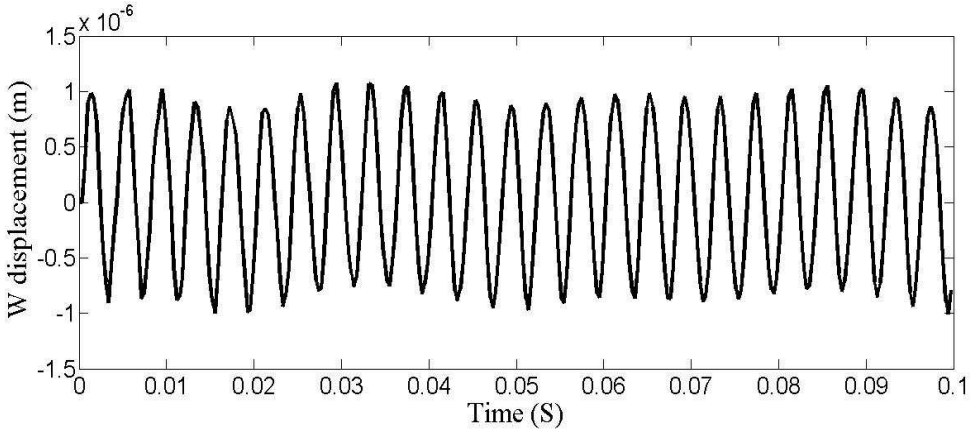

Fig. 5.51: Controlled displacement history in the direction of '*W*' for the quasi-isotropic ply laminated shaft using one actuator.

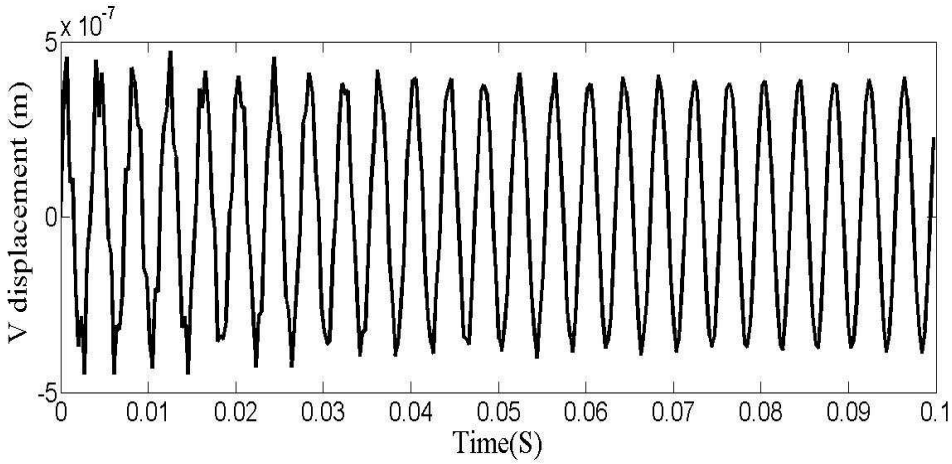

Fig. 5.52: Controlled displacement history in the direction of '*V*' for the quasi-isotropic ply laminated shaft using two actuators.

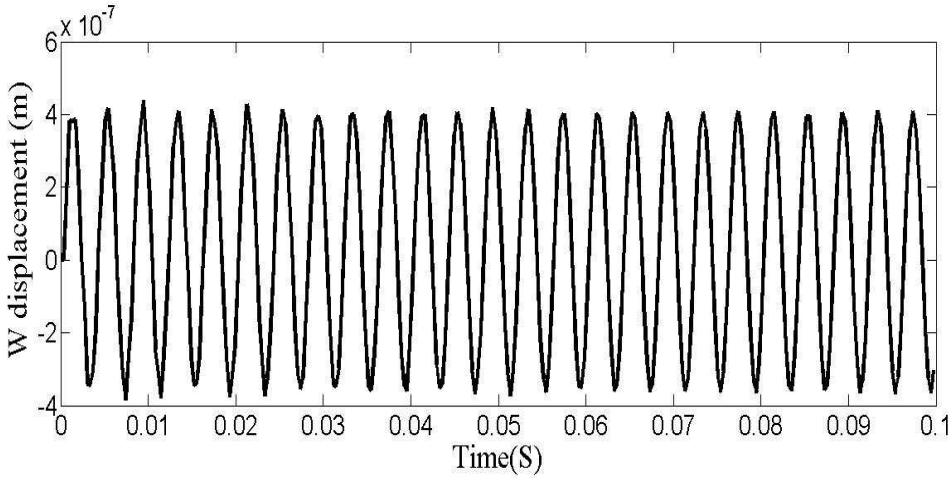

Fig. 5.53: Controlled displacement history in the direction of '*W*' for the quasi-isotropic ply laminated shaft using two actuators.

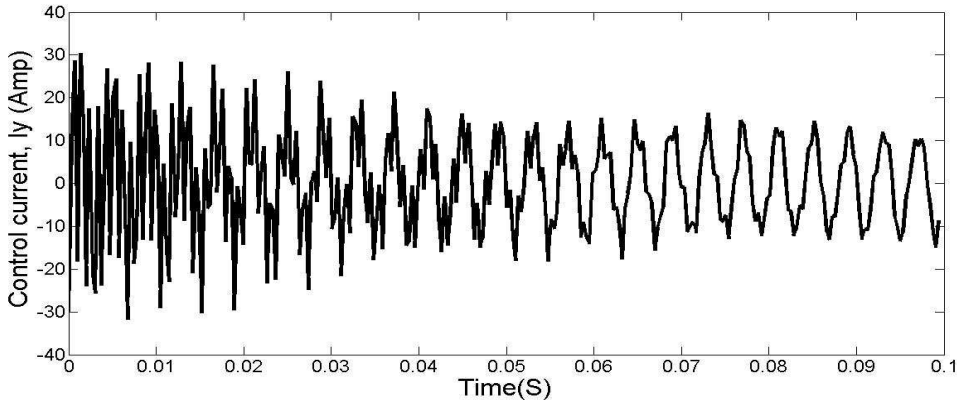

Fig.5.54: Controlled current in the direction of '*Y*' for the quasi-isotropic ply laminated shaft using one actuator.

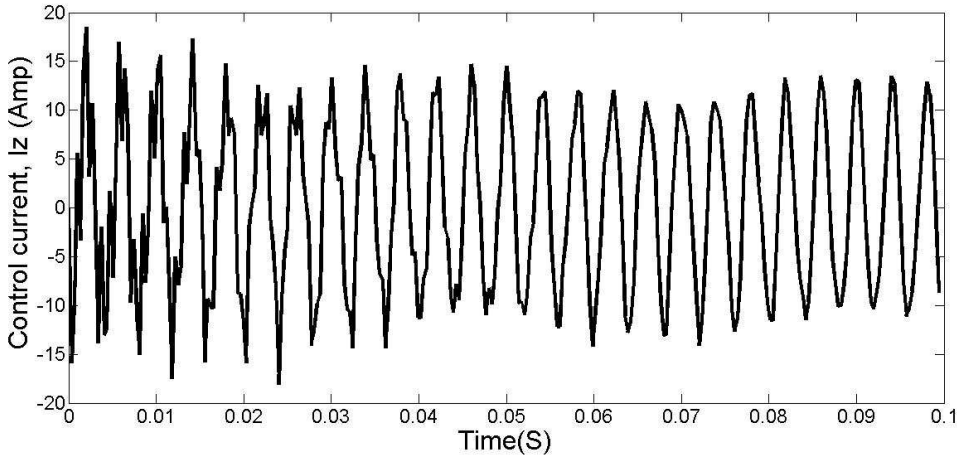

Fig.5.55: Controlled current in the direction of *'Z'* for the quasi-isotropic ply laminated shaft using one actuator.

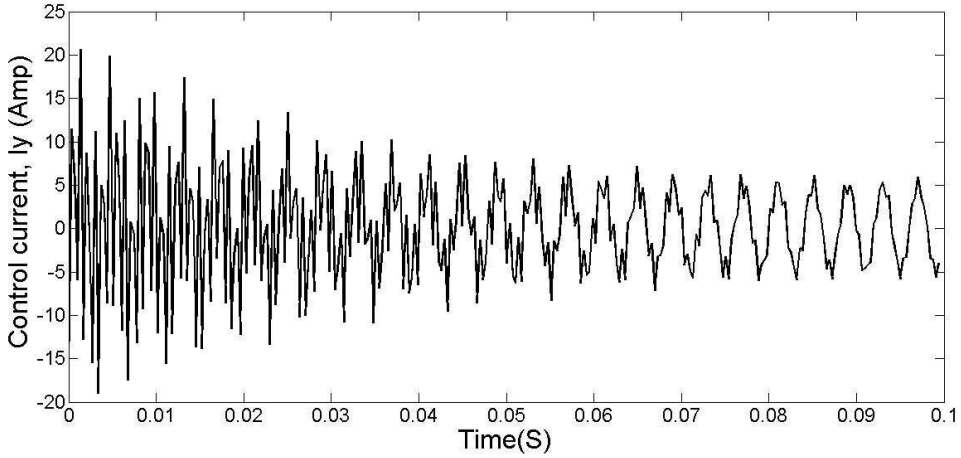

Fig.5.56: Controlled current in the direction of *'Y'* for the quasi-isotropic ply laminated shaft using two actuators.

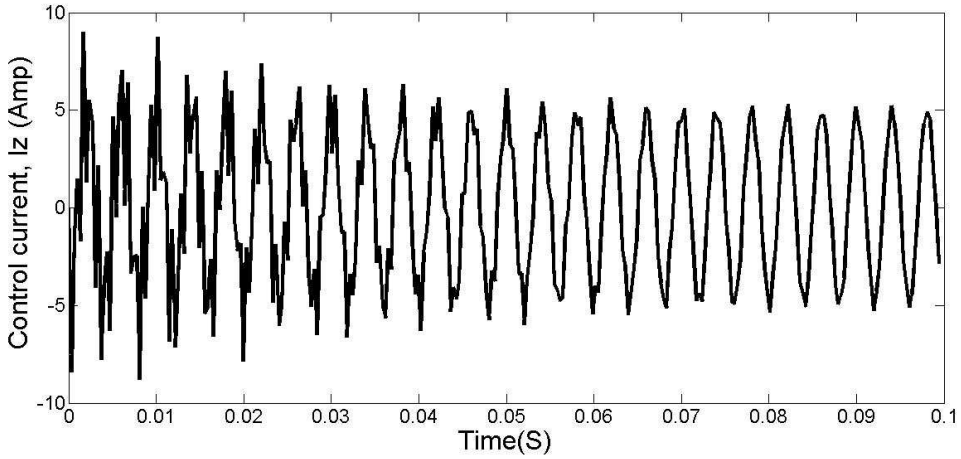

Fig.5.57: Controlled current in the direction of *'Z'* for the quasi-isotropic ply laminated shaft using two actuators.

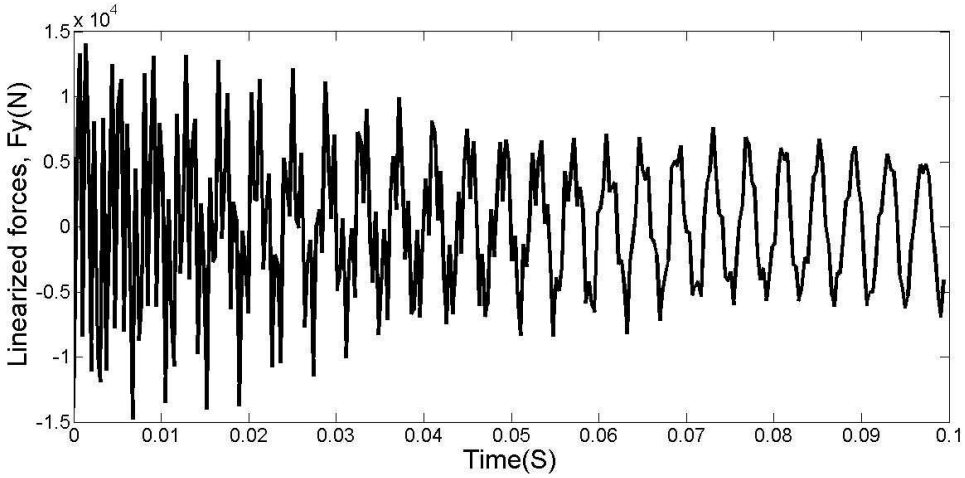

Fig.5.58: Controlled Force in the direction of *'Y'* for the quasi-isotropic ply laminated shaft using one actuator.

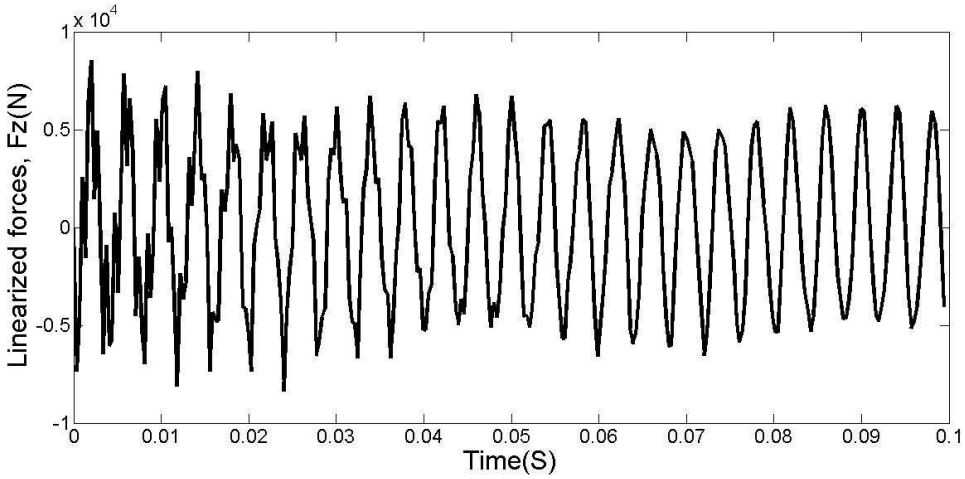

Fig.5.59: Controlled Force in the direction of *'Z'* for the quasi-isotropic ply laminated shaft using one actuator.

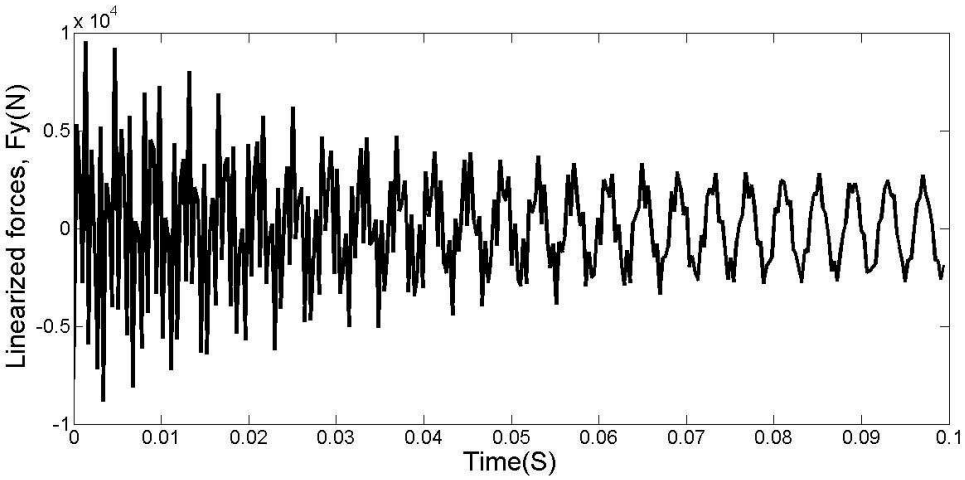

Fig.5.60: Controlled Force in the direction of *'Y'* for the quasi-isotropic ply laminated shaft using two actuators.

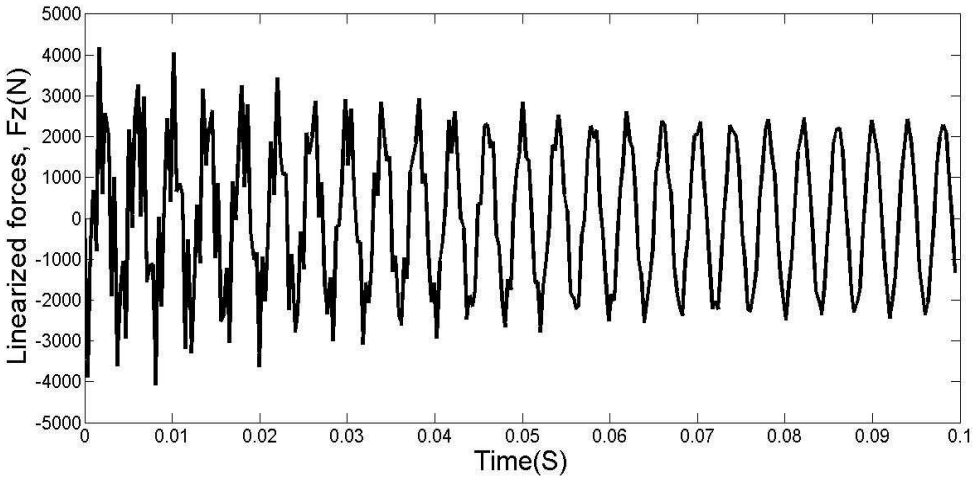

Fig.5.61: Controlled Force in the direction of 'Z' for the quasi-isotropic ply laminated shaft using two actuators.

CHAPTER 6

CONCLUSIONS AND SCOPE OF FURTHER WORK

This chapter presents few important observations based on the active vibration control of composite rotor- shaft system using electromagnetic actuator, PD control scheme using developed MATLAB code. Scope of further work in this direction has also been presented at the end of this chapter

6.1 Conclusions

A three nodded beam element has been used for modeling and vibration analysis of rotating composite shaft. First order shear deformation theory has been employed. The finite element formulation is based on the Timoshenko beam theory. Various types of composite shafts have been considered in order to study the effect of ply orientation on responses of the rotating composite shaft. Active vibration control of the composite shaft has also been implemented using PD control with electromagnetic actuators. The present work enables to arrive at the following important conclusions:

- It has been found that from the Campbell diagram for the four laminated shaft the first critical speed is maximum for the symmetric angle ply with respect to other three plies and it is observed that 3600 r.p.m.
- It has been observed that from the four laminated shaft, the displacement (in both directions) in case of symmetrical angle ply laminated shaft is more than other three.
- The maximum displacement in V direction is found that $1.2x10^{-4}$ m and in the W direction is found that $1.9x10^{-4}$.
- It has also been observed that from the present analysis using two actuators the reduction of response is more than that of single actuator.
- It is found that the reduction of response (in both directions) in case of symmetrical angle ply is more than other thee using two actuators. And it is observed that maximum response is 99.58%, 99.74% in V and W directions.
- Based on control current, maximum control occur using two actuators than that of single actuator. And it has also been observed that maximum control occurs in case of symmetrical angle ply laminated shaft than that of other three and it is found that current requirement in Y and Z directions reduced by 53.12% and 59% respectively using two actuators with respect to single actuator and
- In the same manner maximum control force occur using two actuators than that of single actuator. And it is also observed that maximum control occur in case of symmetrical angle ply laminated shaft than other three and it is found that force requirement in Y and Z directions reduced by 66.66% and 59.09% respectively using two actuators with respect to single actuator.

6.2 Scope of future work

- Optimization for optimal number of actuators and placement of actuators
- Determination of optimal gain parameters
- Determination of induced stress in the lamina/plies of the composite shaft and
- Study of the delamination in the composite plies

REFERENCES

[1] Perini E. A., Bueno D. D., Santos R. B., Junior V. L., Nascimento Luiz de P. "Rotating Machinery Vibration Control Based on Poles Allocation using Magnetic Actuators" International Conference on Engineering Optimization, Rio de Janeiro, Brazil, June (2008), pp.1 -5

[2] Bennett, Stuart "A history of control engineering", (1993).

[3] Ang K.H., Chong G.C.Y., and Li Y. "PID control system analysis, design, and technology", IEEE Trans Control Systems Tech, vol.13, no.4, (2005), pp.559-576.

[4] Foeppl A., Der Civilingenieur, "Das Problem der Delaval'schen Turbinenvelle" (1895), pp. 333-342.

[5] Stodola A., "Neve Kristische Drehzahlen als folye der kreisel wirkuag der laufrader" Gesante Tubinenwes, 15, (1918), PP. 269–275.

[6] Jeffcott H. H., "The lateral vibration of loaded shafts in the neighbourhood of the whirling speeds", Philosophical magazine, vol. 37, (1919), pp.304-315.

[7] Kirk R. G., Gunte E. J., "the effect of support flexibility and damping on the synchronous response of a single mass flexible rotor", J. Eng. Ind., Trans. ASME (1972) pp. 221–232.

[8] Nelson, H.D. and McVaugh, J.M., "The Dynamics of Rotor-bearing Systems Using Finite Elements," ASME Journal of Engineering for Industry, Vol. 98,No.2, (1976), pp. 593-600.

[9] Yamamoto T., Yasuada K., and Nagasaka I. "Ultra-Subharmonic oscillations in a nonlinear vibratory system" Bulletin of the JSME, 19(138), (1976), pp.1442-1447.

[10] Holmes A. G., Ettles C. M., and Mayes L. W., "Aperiodic behaviour of a rigid shaft in short journal bearings" International Journal for Numerical methods in Engineering,vol. 12, (1978), pp. 695-702,

[11] Panda K. C. and Dutt J. K., "Design of Optimum Support Parameters for Minimum Rotor Respons and Maximum Stability Limit.",Journal of Sound and Vibration, vol. 223 (1), (1999) , pp. 1- 21, 2409, June 10–14, (1985), pp. 317–326.

[12] Cunningham R.E.,"Steady-state unbalance response of a three-disk flexible rotor on flexible,damped supports", ASME J. Mech. Des.100, (1978), pp.563-573.

[13] Stanway R., and Burrows C.R., "Active vibration control of flexible rotor on flexible-mounted journal bearings", ASME Journal of Dynamical Systems, Measurement and control 103, (1981), pp. 383-388.

[14] Viderman Z., and Porat I., "An optimal control method for passage of a flexible rotor through resonances" ASME journal of dynamics systems, measurement and control, vol. 109, (1987).

[15] Subbiah R. and Rieger N. "On the transient analysis of rotor bearing systems" (1988), ASME Journal of "Vibration, Acoustics, Stress and Reliability in Design", vol. 110.

[16] Dutt J. K., Nakra B. C., "Vibration reduction of rotor shaft systems using viscoelastic polymeric supports", J. Vibr. Acoust., Trans. ASME 115, (1993), pp. 221–223.

[17] Chen T. Y., and Wang B. P., "Optimum Design of Rotor-Bearing System with Eigen value Constraints", Journal of Engineering for Gas Turbines and Power, vol. 115, (1993), pp. 256- 260.
[18] Childs D.W., "Turbo machinery Rotor dynamics, Phenomena, Modelling, and Analysis", John Wiley & Sons Inc, (1993).
[19] Wettergren H. L., Olsson K. O., "Dynamic Instability of a rotating asymmetric shaft withinternal viscous damping supported on anisotropic bearings", J. Sound Vibr. 195 (1) (1996), pp.75-84.
[20] Chang M. Y., Chen J. K., Chang C. Y. "A simple spinning laminated composite shaft model", International Journal of Solids and Structures **41**, (2004), pp. 637–662.
[21] Zinberg H. and Symonds M. F. "The development of an advanced composite tail rotor driveshaft", In 26th Annual Forum of the American helicopter Society, volume Washington, DC, (1970).
[22] Dos Reis H. L. M., Goldman R. B., and. Verstrate P. H. "Thin walled laminated composite cylindrical tubes" Part III - critical speed analysis, Journal of Composites Technology and Research, vol. 9, (1987), pp. 58-62.
[23] Gupta K. and Singh S. E. " Dynamics of composite rotors", In Proceedings of Indo-US symposium on Emerging Trends in Vibration and Noise Engineering, New Delhi, India, (996), pp. 59-70.
[24] Kim C. D. and Bert C. W. "Critical speed analysis of laminated composite and hollow drive shafts. Composites Engineering, vol. 3, (1993), pp. 633-643.
[25] Bert C. W. and Kim C. D. "Dynamic instability of composite-material drive shaft subjected to fluctuating torque and/or rotational speed" Dynamics and Stability of Systems, vol. 2, (1995) pp. 125-147.
[26] Chang C.-Y., Chang M.-Y., and Huang J. H., "Vibration analysis of rotating composite shafts containing randomly oriented reinforcements," Composite Structures, vol. 63, no. 1, (2004), pp. 21–32.
[27] Pilkey W.D., "Efficient optimal design of suspension system for rotating shafts", Journal ofApplied Mechanics Transactions of the American Society of Mechanical Engineers 98 (3) (1976), pp. 1026–1029.
[28] Muszynska A., "Vibrational diagnostics of rotating machinery malfunctions", Int. J. Rotat. Mach. 1 (3–4), (1995), pp. 237–266.
[29] Wettergren H.L., Olsson K.O., "Dynamic Instability of a rotating asymmetric shaft withinternal viscous damping supported on anisotropic bearings", J. Sound Vibr. 195 (1) (1996), pp.75-84.
[30] Lalanne M. and Ferraris G., "Rotor Dynamics Predictions in Engineering", John Wiley and Sons, (1998).
[31] DOI J. H. Hutchison, "Shear Coefficients for Timoshenko Beam Theory", Journal of Applied Mechanics, January, (2001).
[32] Gustavsson R., "Modelling and Analysis of Hydropower Generator Rotors", Licentiate Thesis, Lulea University of Technology, (2005).
[33] Nighil M.C., Dutt J.K., Irretier H., " Rotor vibration control with electro-magnetic exciter", Paper ID: 291, in: Proceedings of the IFTOMM conference on Rotor

Dynamics, held at Vienna Institute of Technology Austria from 25th to 28th September (2006).

[34] Chang-Jian, Cai-Wan and Chen Chao-Kuang "Bifurcation and chaos analysis of a flexible rotor supported by turbulent long journal bearings", Chaos, Solutions and Fractals, 34, (2007), pp. 1160-1179.

[35] Bueno D. D., "Controle Ativo de Vibrações e Localização Ótima de Sensores e Atuadores Piezelétricos, Dissertação de Mestrado (Engenharia Mecânica)" – Faculdade de Engenharia, Universidade Estadual Paulista, Ilha Solteira, (2007).

[36] Das, A.S., Nighil, M.C., Dutt, J.K. and Irretier, H., "Vibration Control and Stability Analysis of Rotor-Shaft System with Electromagnetic Exciters," Mechanism and Machine Theory, 43, (2008), pp. 1295–1316.

[37] Das A.S., Dutt J.K., Ray K., "Active vibration control of unbalanced flexible rotor–shaft systems parametrically excited due to base motion" Applied Mathematical Modelling 34 (2010) pp. 2353–2369

[38] Schweitzer G., Bleuler H.A. "Traxler, Active Magnetic Bearings", (1994).

[39] Schweitzer G., "Magnetic bearing for vibration control", in: NASA Conference publication.

[40] Schittenhelm R. S., Borsdorf M., Riemann B., Rinderknecht S. "Linear Quadratic Regulation of a Rotating Shaft being Subject to Gyroscopic Effect" WCECS 2012, October 24-26, San Francisco, USA, (2012).

[41] Maslen E., "Magnetic bearings", University of Virginia, Department of Mechanical, Aerospace, and Nuclear Engineering, Charlottesville, Virginia, USA, June, (2000).

[42] Blanco-Ortega A., Beltrán-Carbaja F., and Silva-Navarro G. "Active Disk for Automatic Balancing of Rotor-Bearing Systems. American Control Conference", ACC2008. ISBN: 978-1-4244-2078-0. (2008).

[43] Guozhi Y. Fah Y. F., Guang C. Guang M., Tong F., Yang Q. " Electro-rheological multi-layer squeeze film damper and its application to vibration control of rotor system" Journal of Vibration and Acoustics, Vol. 122, ISSN: 1048-9002. (2000), pp. 7-11.

[44] Jinhao Q. Tani J. and T. "Kwon Control of self-excited vibration of a rotor system with active gas bearings", Journal of Vibration and Acoustics, Vol. 125, ISSN: 1048-9002. (2003), pp. 328-334.

[45] Palazzolo B., Jagannathan S., Kaskaf A. F., Monatgue G. T., Kiraly L. J. "Hybrid active vibration control of rotorbearing systems using piezoelectric actuators", Journal of Vibration and Acoustics, Vol. 115, ISSN: 1048-9002, (1993), pp. 111-119.

[46] Sheu. G., Yang S. and Yang C. "Design of experiments for the controller of rotor systems with a magnetic bearing" Journal of Vibration and Acoustics, Vol. 119, No. 2, , ISSN: 1048-9002, (1997), pp.200-207.

[47] Zhou S. and Shi J. "Active balancing and vibration control of rotating machinery" a survey, The Shock and Vibration Digest, Vol. 33, ISSN: 0583-1024, (2001), pp.361-371.

[48] Lee S. Kim B., Moon J., Kim D. "A study on active balancing for rotating machinery using influence coefficient method", Proceedings of International Symposium on Computational Intelligence in Robotics and Automation. Espoo, Finland, ISBN: 0-7803-9356-2, (2005), pp. 659- 664.

[49] Yu, X "General influence coefficient algorithm in balancing of rotating machinery", International Journal of Rotating Machinery, Vol. 10, ISSN: 1023-621X, (2004), pp.85-90.

[50] Zhou S., Dyer S., Shin, J. Shi K. K., Ni J. "Extended influence coefficient method for rotor active balancing during acceleration", Journal of Dynamics Systems, Measurements and Control, Vol. 126, ISSN: 0022-0434, pp. 219-223.

[51] Ljung L. "Systems identification: theory for the user" Englewood Cliffs, NJ: Prentice-Hall, ISBN-13: 978-0136566953, (1987), pp. 168-361.

[52] Sagara, S. and Zhao Z. Y. "Recursive identification of transfer function matrix in continuous systems via linear integral filter", International Journal of Control, Vol. 50, ISSN: 0020-7179, (1989), pp.457-477.

[53] Sagara S. and Zhao Z. Y. "Numerical integration approach to on-line identification of continuous systems", Automatica, Vol. 26, ISSN: 0005-1098, (1990), pp.63-74.

[54] Lund J.W., "Response characteristics of a rotor with flexible damped supports, dynamics of Rotor", Proceedings of the IUTAM Symposium, Springer-Verlag, Lyngby, Denmark, (1974), pp. 2–16.

[55] Allaire P.E., Humphris R.R., and Kelm R.D., "Rotordynamic instability problems in high-performance turbomachinery", NASA CP-2443, "Dynamics of a flexible rotor in magnetic bearings", (1986), pp. 419-430.

[56] Koroishi E.H., Steffen Jr. V., "Active vibration control using electromagnetic actuator: A simple model approach (Conferencia Brasileira control application)", (2011), pp. 51-54.

[57] Koroishi E. H. , Steffen Jr V. and Mahfoud J. " Fuzzy Control of Rotor System Using an Electromagnetic Actuator" Owned by the authors, published by EDP Sciences, 09003, (2012), pp. 1-6.

[58] Keith F. J. and Allaire P. "Digital control of magnetic bearings supporting a multimass flexible rotor", (1990), Tribology transactions, 33.

[59] Cheung L. Y., Dunn R.W., Daniels A. R. and Berry T. "Active vibration control of rotor systems". (1994), Control 94, IEEE, pp. 1157-1163.

[60] Abduljabbar Z., ELMadany M.M., and AlAbdulwahab A.A. "Computers and Structures", 58 (3), pp.499-511 "Active Vibration Control of a Flexible Rotor", (1996), pp. 75–84.

[61] Roy T., Chakaraborty D. "Optimal vibration control of smart fiber reinforced composite shell structures using improved genetic algorithm" Journal of Sound and Vibration 319 (2009) pp.15–40

[62] Cole M.O.T., Keogh P.S., Burrows C.R., "Control of multi-frequency rotor vibration Components", J. Mech. Eng. Sci., Proc. I. Mech. E C-216 (2002) pp. 165–177.

[63] Jingjun Zhang, Lili He, Ercheng Wang, Ruizhen Gao Hebei "Workshop on Computational Intelligence and Industrial Application", University of Engineering, Handan, Hebei, 05, China, IEEE Pacific-Asia, (2008), pp 60-38,.

[64] Koroishi E. H., Perini E. A., Nascimento L. P., Lopes jr V., Steffen jr V., "Active Vibration Control in Rotor System Using Magnetic Bearing with LQR", Proceedings of the 1st International Congress of Mathematics, Engineering and Society-ICMES 2009.

[65] Janik T.K., Irretier H., "New excitation and response measurement techniques for modal testing of flexible rotors", Proceedings of the IFTOMM Conference on Rotordynamics, Darmstadt, (1998), pp. 695–708.
[66] Dutt J.K., Toi T.,"Rotor vibration reduction with polymeric sectors", J. Sound Vibr., 262 (4), (2003), pp. 769 -793.
[67] Meirovitch L. "Dynamics and Control of Structures", Wiley Interscience, Bracksburg, VA, USA.

❖ List of publication from the present work:

- Sikandar Kumar, D. Koteswara Raoand, Tarapada Roy "Active Vibration Control of Layered Composite Rotor Shaft System Using Electromagnetic Actuator" 1st world conf. of WCFMAAE, IIT Delhi, 2nd February, 2013